Electronic Supplementary Material (ESI) for RSC Advances.

Supplementary Information

Ion-pair recognition of amidinium salts by partially hydrogen-bonded heteroditopic cyclo[6]aramide

Shanshan Shi, Yumin Zhu, Xiaowei Li, Xiangyang Yuan,

Teng Ma, Wenli Yuan, Guohong Tao, Wen Feng and Lihua Yuan*

College of Chemistry, Key Laboratory for Radiation Physics and Technology of Ministry of Education, Institute of Nuclear Science and Technology, Sichuan University, Chengdu 610064, China

E-mail: lhyuan@scu.edu.cn
Fax: +86 28 85418755; Tel: +86-28-85412890

Contents

1. Synthesis of heteroditopic cyclo[6]aramides 1a

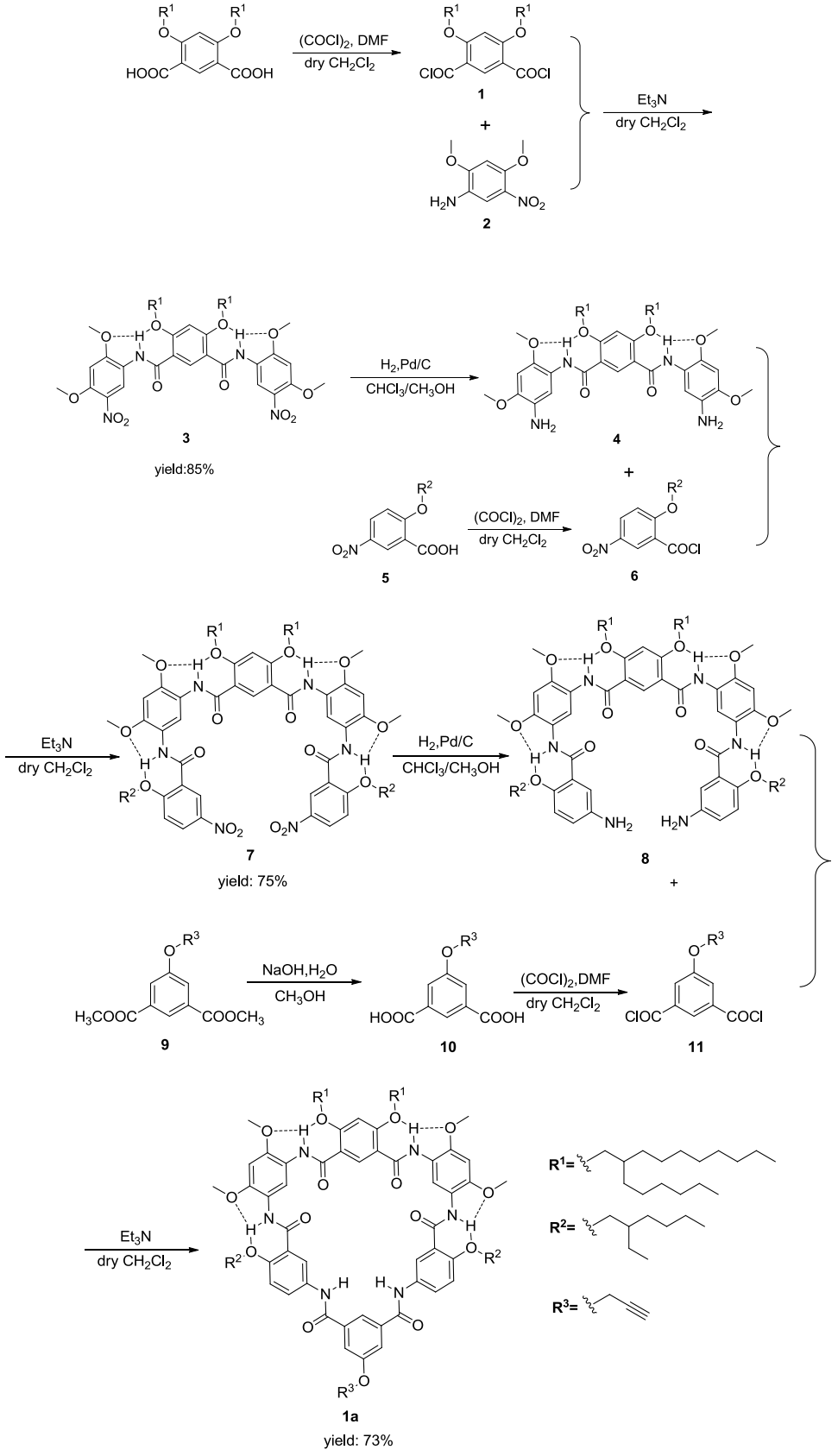

Scheme S1. Synthetic routes for heteroditopic cyclo[6]aramides **1a**.

Cyclo[6]aramide **1a** was synthesized following a literature procedure.[S1]

Compounds **3** and **7** were converted into **4** and **8**, respectively by catalytic hydrogenation. Compounds **4** and **8** were used directly in the subsequent reaction without further purification.

Compounds **3**[S2], **5**[S3] and **10**[S4] were synthesized according to an analogous literature procedure.

2. ^{1}H NMR spectra of new compounds

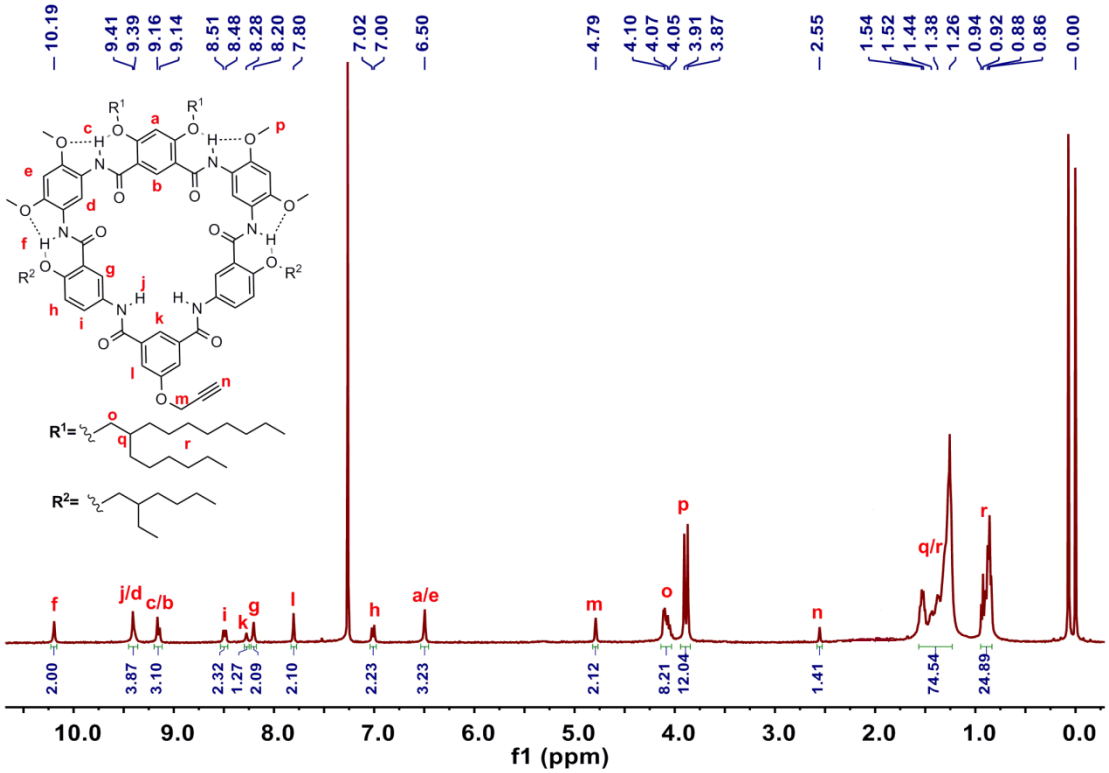

Figure S1. ^{1}H NMR spectrum of cyclo[6]aramide **1a** (400 MHz, $CDCl_3$, 298 K).

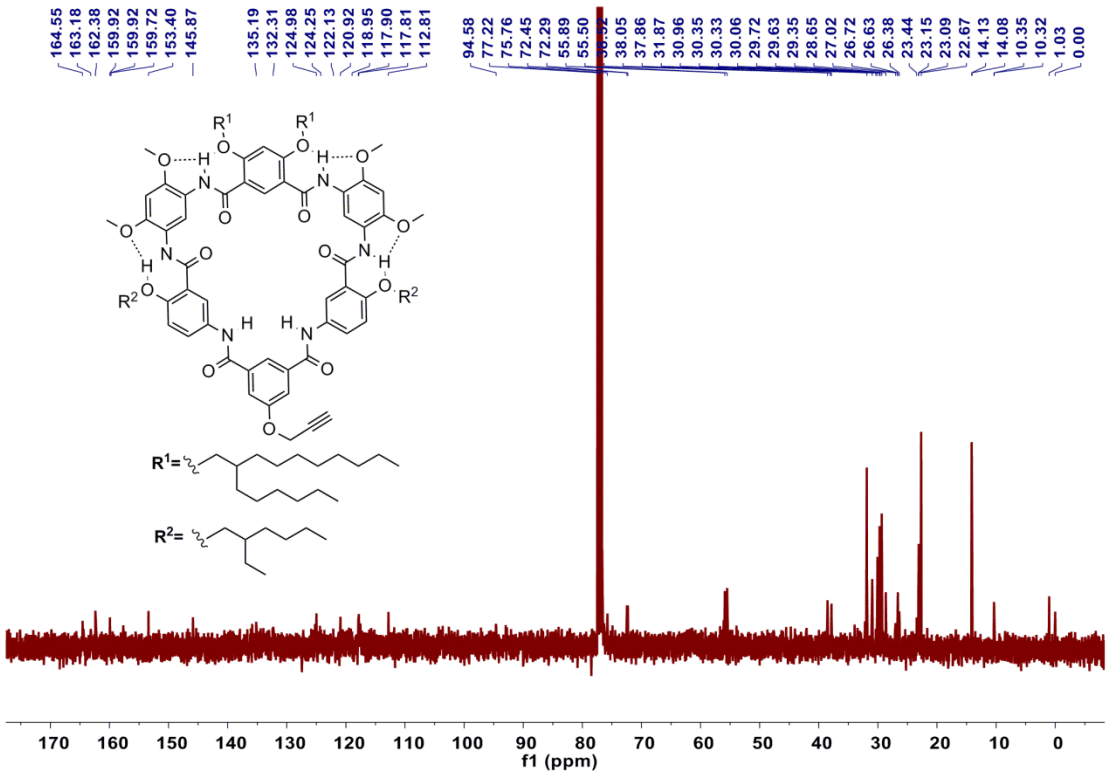

Figure S2. ^{13}C NMR spectrum (101 MHz, $CDCl_3$) of cyclo[6]aramide **1a** at 298 K.

3. Host-guest complexation of 1a and G1, G6 and G7

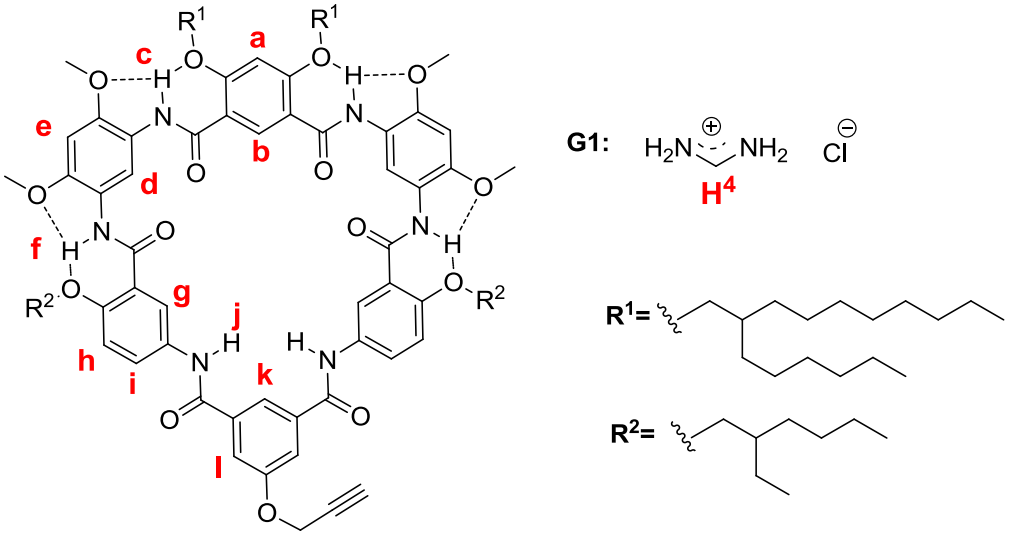

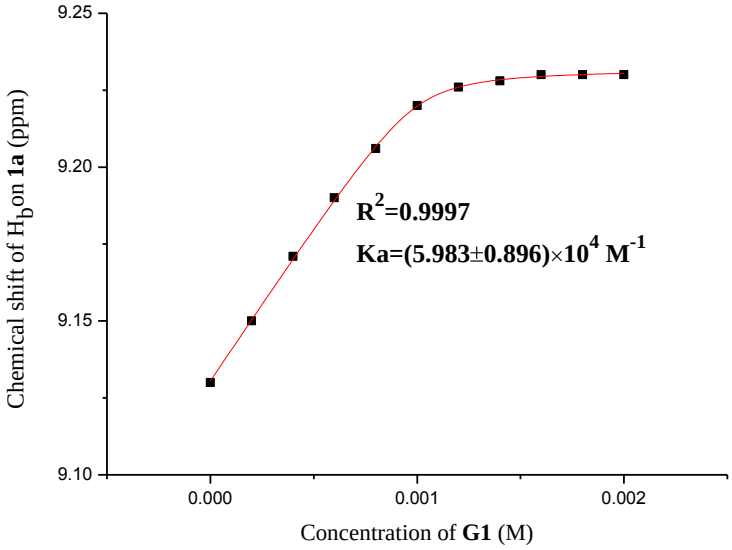

Figure S3. Determination of the binding constant of **1a•G1** in $CDCl_3$-CD_3OD (v/v, 9:1) at 298 K. Fitting result based on H_b of **1a**.

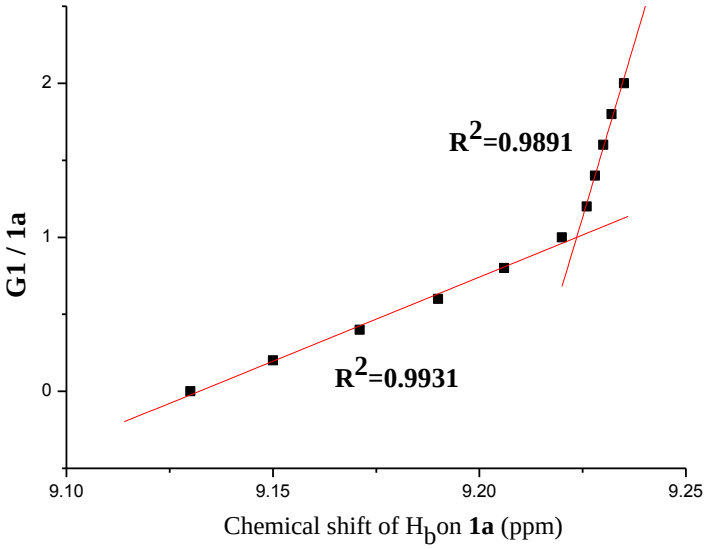

Figure S4. Mole ratio plot for the complexation between **1a** and **G1**, indicating a 1:1 stoichiometry.

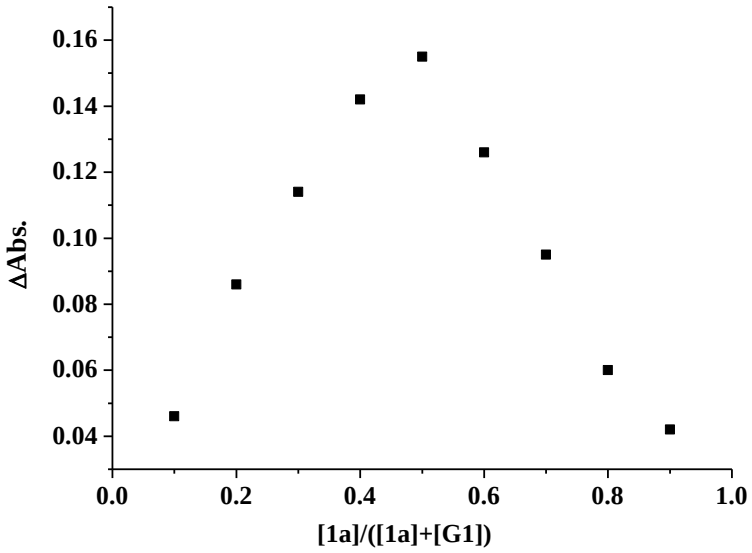

Figure S5. Job's plot for the complexation of **1a** and **G1** in $CDCl_3$-CD_3OD (v/v, 9:1) based on the absorbance at 365 nm, indicating a 1:1 stoichiometry. The total concentration is 3×10^{-4} M.

Table S1. The chemical shifts δ (ppm) for the 1:1 solution of **1a** and **G1** in $CDCl_3$-CD_3OD (v/v, 9:1).

Protons	**1a**	**1a**+**G1**	
	δ_f (ppm)	δ_b (ppm)	$\Delta\delta=\delta_b-\delta_f$ (ppm)
H_c	9.26	9.49	0.23
H_b	9.12	9.23	0.11
H_d	9.42	9.39	-0.03
H_f	10.32	10.45	0.13
H_g	8.02	8.48	0.46
H_k	8.23	8.89	0.66

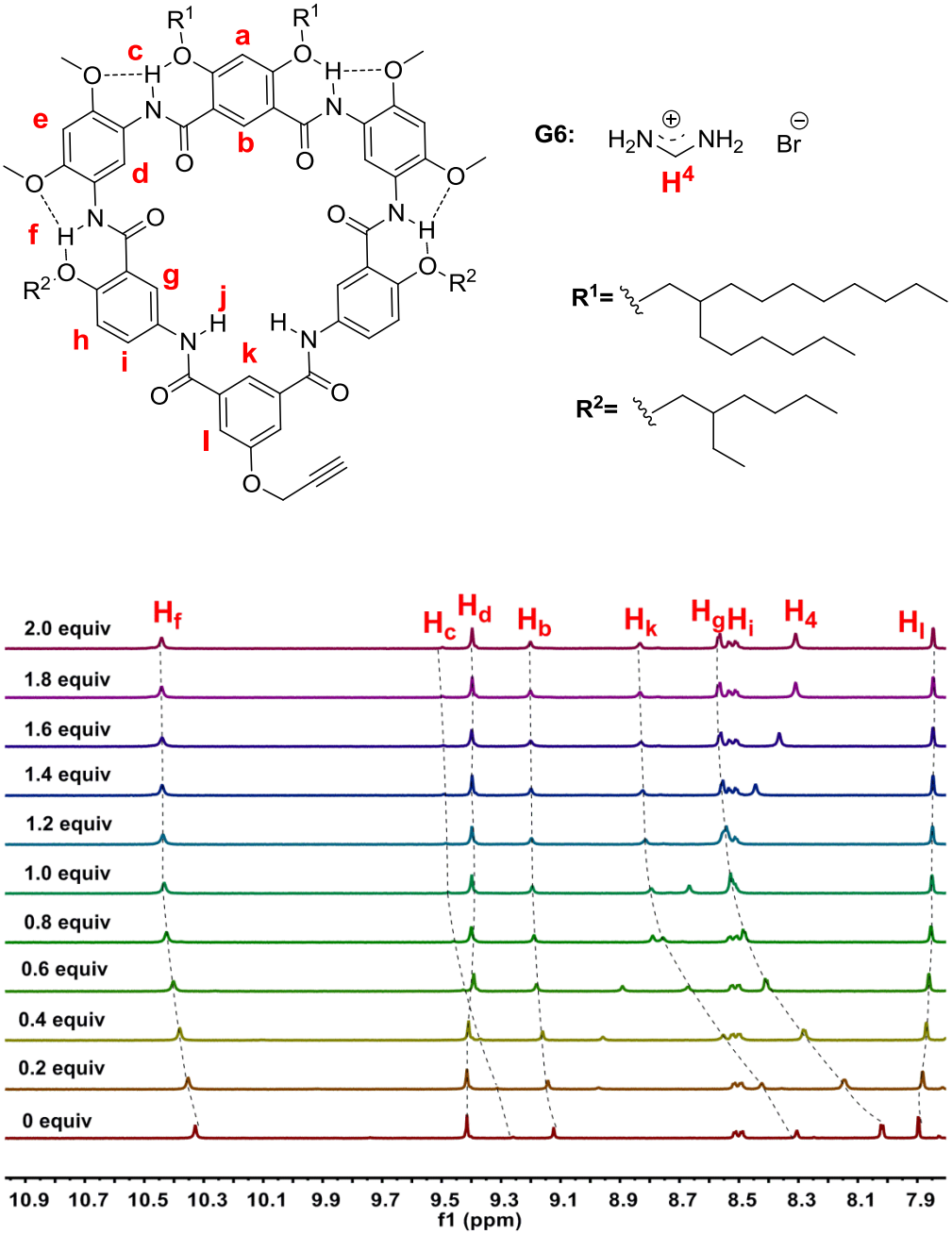

Figure S6. Partial stacked ^{1}H NMR spectra (400 MHz, 298 K) of cyclo[6]aramide **1a** (1.0 mM) titrated by **G6** (0-2.0 equiv) in $CDCl_3$-CD_3OD (v/v, 9:1).

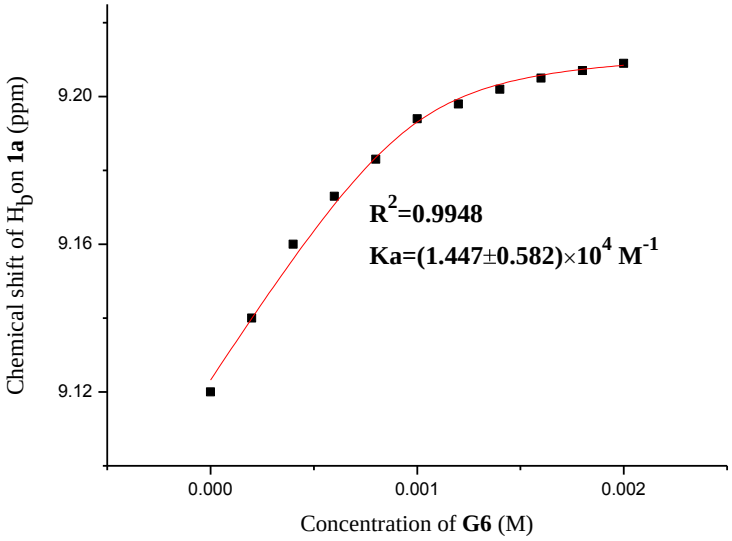

Figure S7. Determination of the binding constant of **1a•G6** in $CDCl_3$-CD_3OD (v/v, 9:1) at 298 K. Fitting result based on H_b of **1a**.

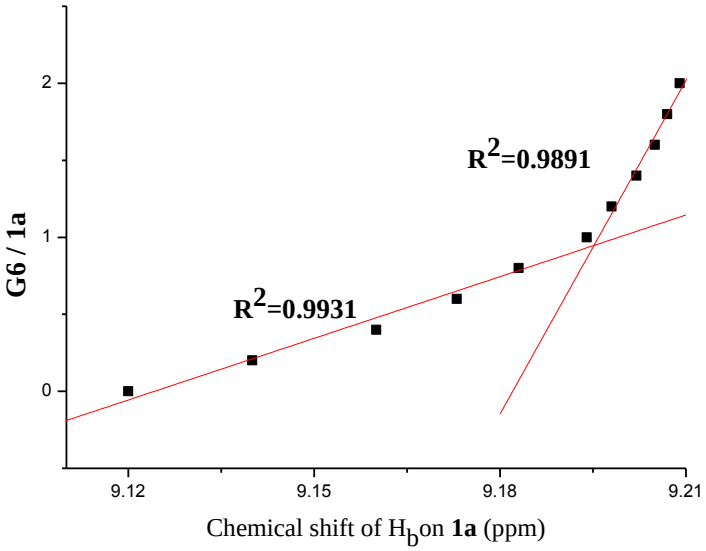

Figure S8. Mole ratio plot for the complexation between **1a** and **G6**, indicating a 1:1 stoichiometry.

Table S2. The chemical shifts δ (ppm) for the 1:1 solution of **1a** and **G6** in $CDCl_3$-CD_3OD (v/v, 9:1).

Protons	**1a**	**1a**+**G6**	
	δ_f (ppm)	δ_b (ppm)	$\Delta\delta=\delta_b-\delta_f$ (ppm)
H_c	9.26	9.48	0.22

H_b	9.12	9.20	0.08
H_d	9.42	9.40	-0.02
H_f	10.32	10.44	0.12
H_g	8.02	8.50	0.48
H_k	8.23	8.83	0.60

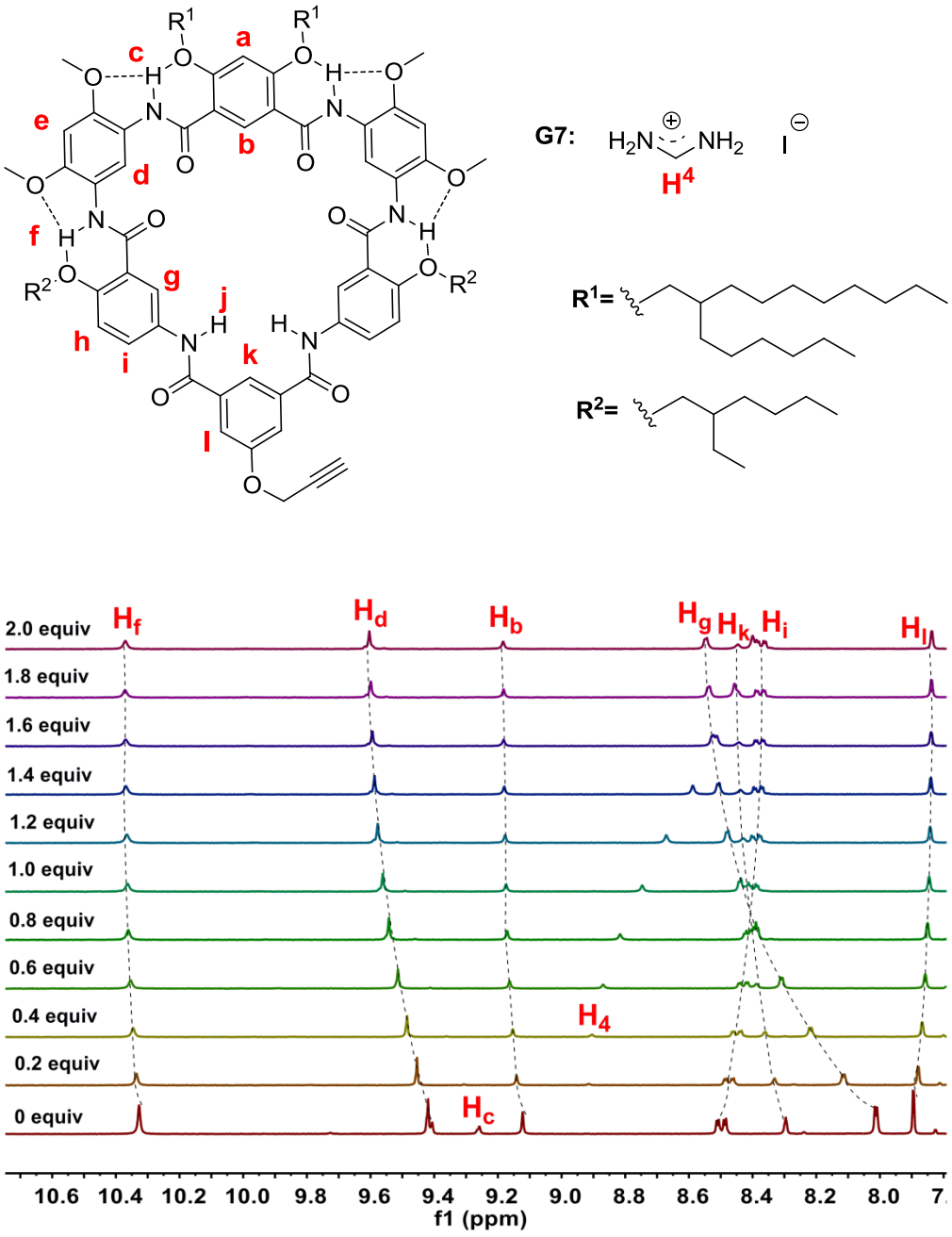

Figure S9. Partial stacked ^{1}H NMR spectra (400 MHz, 298 K) of cyclo[6]aramide **1a** (1.0 mM) titrated by **G7** (0-2.0 equiv) in $CDCl_3$-CD_3OD (v/v, 9:1).

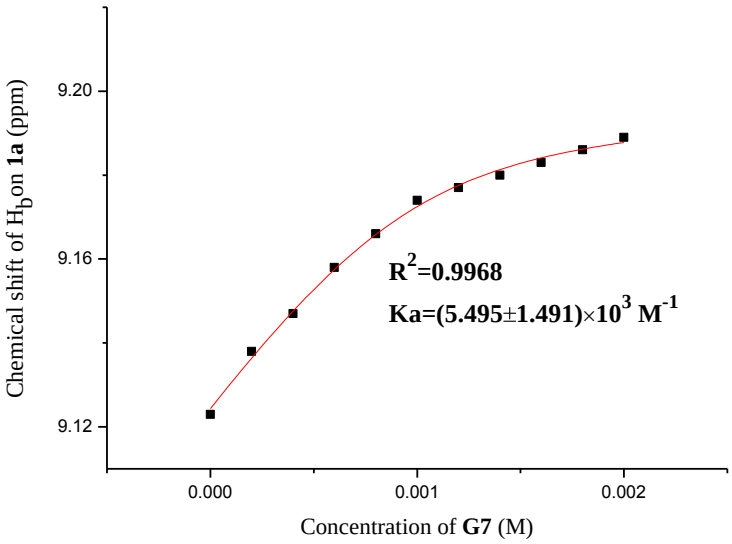

Figure S10. Determination of the binding constant of **1a•G7** in $CDCl_3$-CD_3OD (v/v, 9:1) at 298 K. Fitting result based on H_b of **1a**.

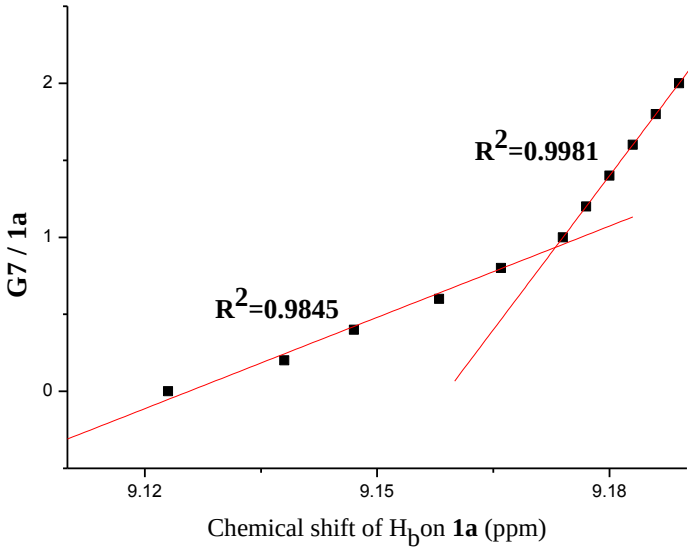

Figure S11. Mole ratio plot for the complexation between **1a** and **G7**, indicating a 1:1 stoichiometry.

Table S3. The chemical shifts δ (ppm) for the 1:1 solution of **1a** and **G7** in $CDCl_3$-CD_3OD (v/v, 9:1).

Protons	**1a**	**1a+G7**	
	δ_f (ppm)	δ_b (ppm)	$\Delta\delta=\delta_b-\delta_f$ (ppm)
H_b	9.12	9.19	0.07

H_d	9.42	9.60	0.18
H_f	10.32	10.37	0.05
H_g	8.02	8.52	0.50
H_k	8.23	8.45	0.22

4. Host-guest complexation of 1a and G2

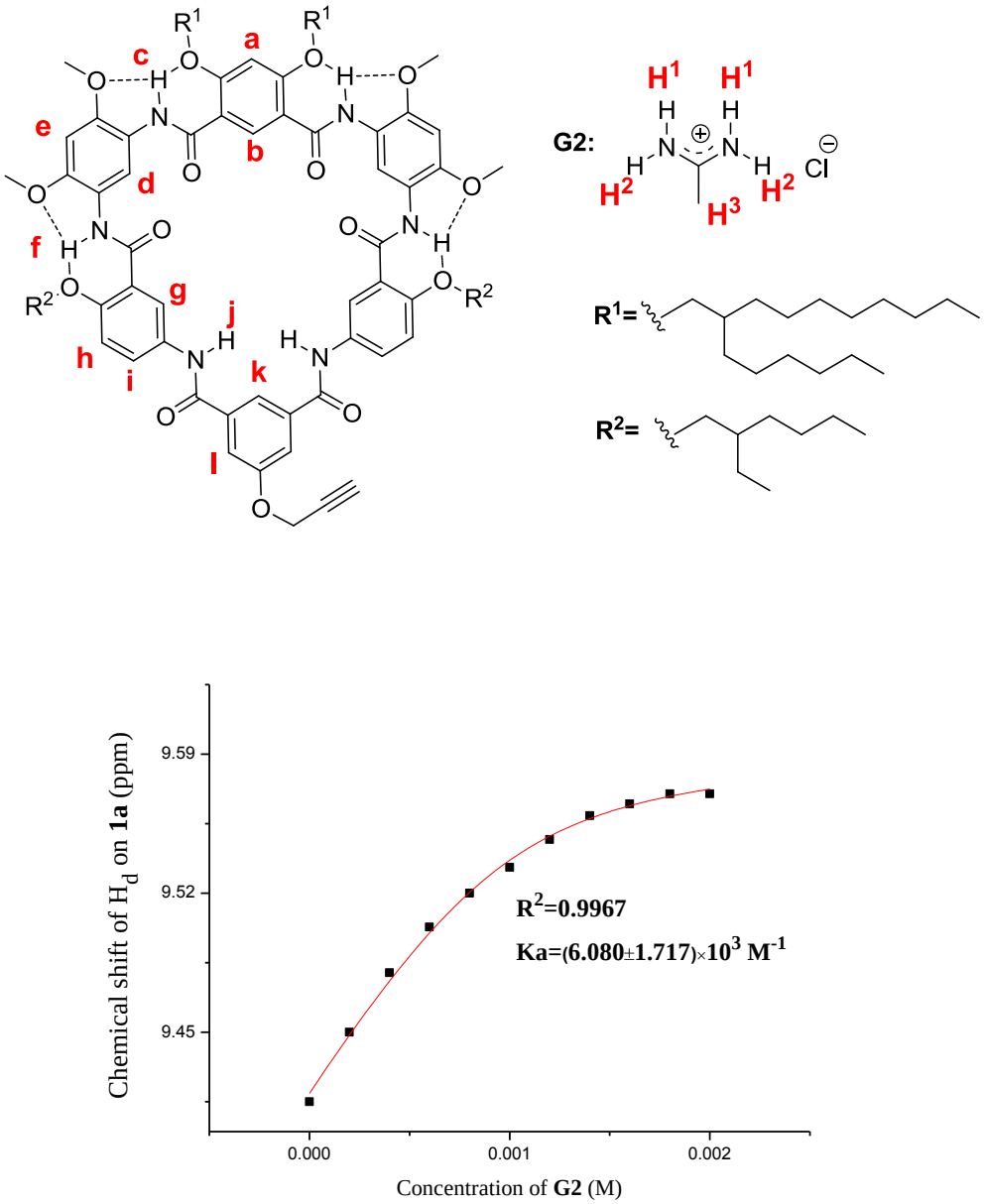

Figure S12. Determination of the binding constant of **1a•G2** in $CDCl_3$-CD_3OD (v/v, 9:1) at 298 K. Fitting result based on H_d of **1a**.

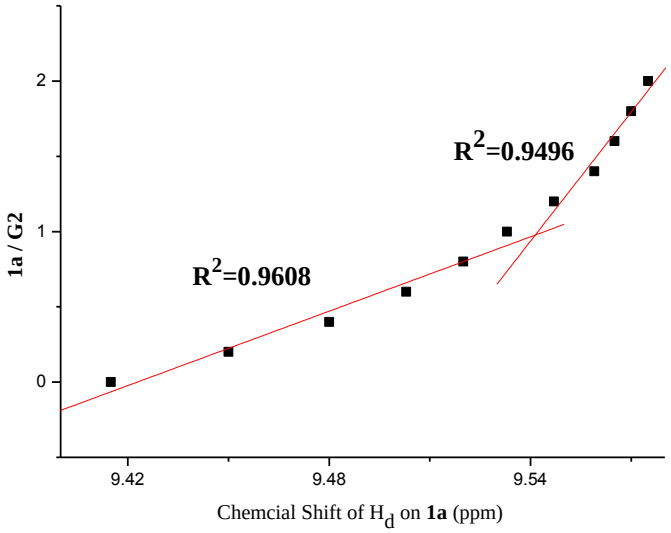

Figure S13. Mole ratio plot for the complexation between **1a** and **G2**, indicating a 1:1 stoichiometry.

Table S4. The chemical shifts δ (ppm) for the 1:1 solution of **1a** and **G2** in $CDCl_3$-CD_3OD (v/v, 9:1).

Protons	**1a**	**1a+G2**	
	δ_f (ppm)	δ_b (ppm)	$\Delta\delta=\delta_b-\delta_f$ (ppm)
H_b	9.12	9.07	-0.05
H_d	9.42	9.57	0.15
H_g	8.02	8.36	0.34
H_i	8.51	8.33	-0.18
H_k	8.23	8.31	0.08

5. Host-guest complexation of 1a and G3

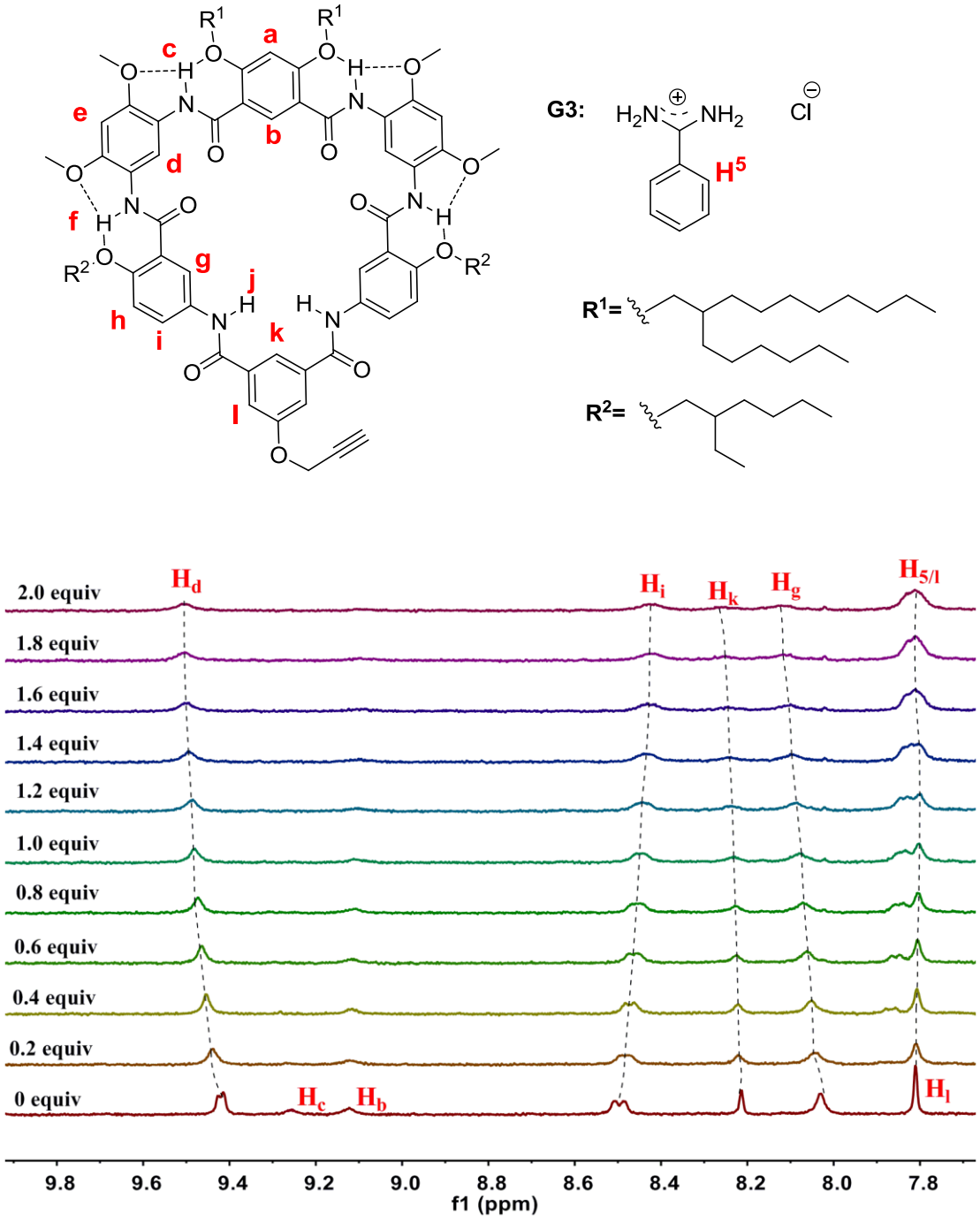

Figure S14. Partial stacked ^{1}H NMR spectra (400 MHz, 298 K) of cyclo[6]aramide **1a** (1.0 mM) titrated by **G3** (0-2.0 equiv) in $CDCl_3$-CD_3OD (v/v, 9:1).

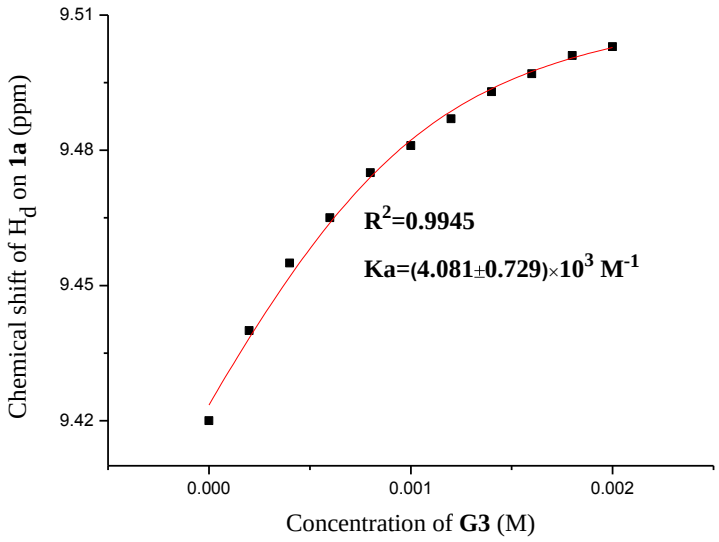

Figure S15. Determination of the binding constant of **1a•G3** in $CDCl_3$-CD_3OD (v/v, 9:1) at 298 K. Fitting result based on H_d of **1a**.

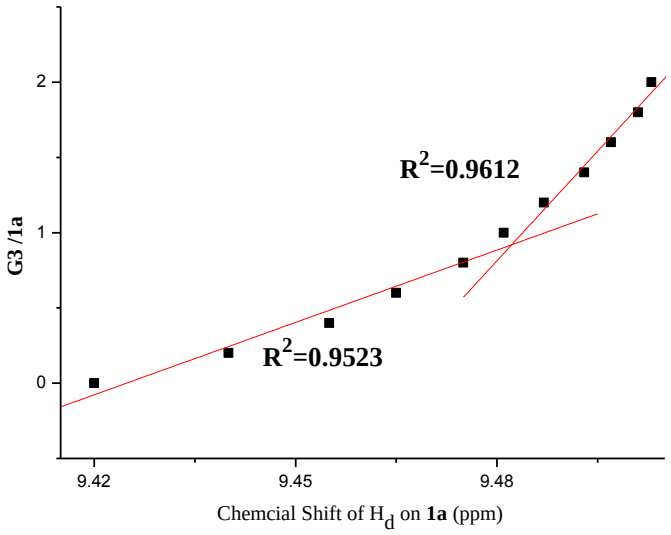

Figure S16. Mole ratio plot for the complexation between **1a** and **G3**, indicating a 1:1 stoichiometry.

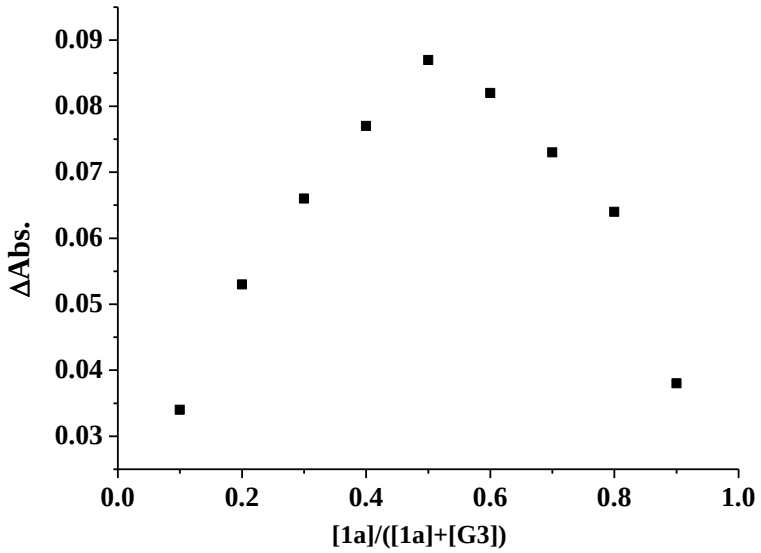

Figure S17. Job's plot for the complexation of **1a** and **G3** in $CDCl_3$-CD_3OD (v/v, 9:1) based on the absorbance at 365 nm, indicating a 1:1 stoichiometry. The total concentration is 3×10^{-4} M.

Table S5. The chemical shifts δ (ppm) for the 1:1 solution of **1a** and **G3** in $CDCl_3$-CD_3OD (v/v, 9:1).

Protons	**1a**	**1a+G3**	
	δ_f (ppm)	δ_b (ppm)	$\Delta\delta=\delta_b-\delta_f$ (ppm)
H_b	9.12	9.10	-0.02
H_d	9.42	9.50	0.08
H_g	8.02	8.12	0.10
H_i	8.51	8.42	-0.11
H_k	8.23	8.31	0.08

6. Host-guest complexation of 1a and G4

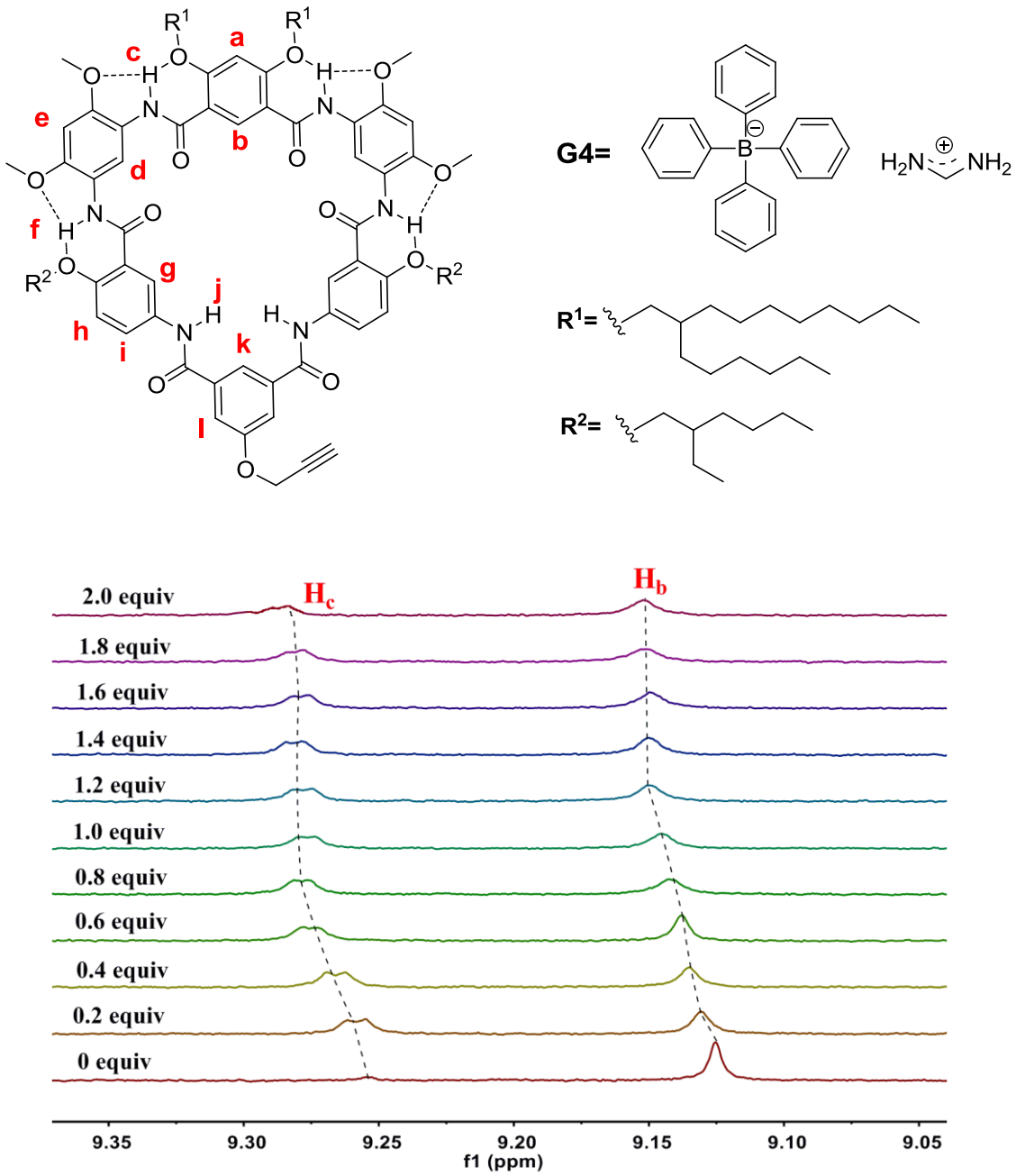

Figure S18. Partial stacked ^{1}H NMR spectra (400 MHz, 298 K) of cyclo[6]aramide **1a** (1.0 mM) titrated by **G4** (0-2.0 equiv) in $CDCl_3$-CD_3OD (v/v, 9:1).

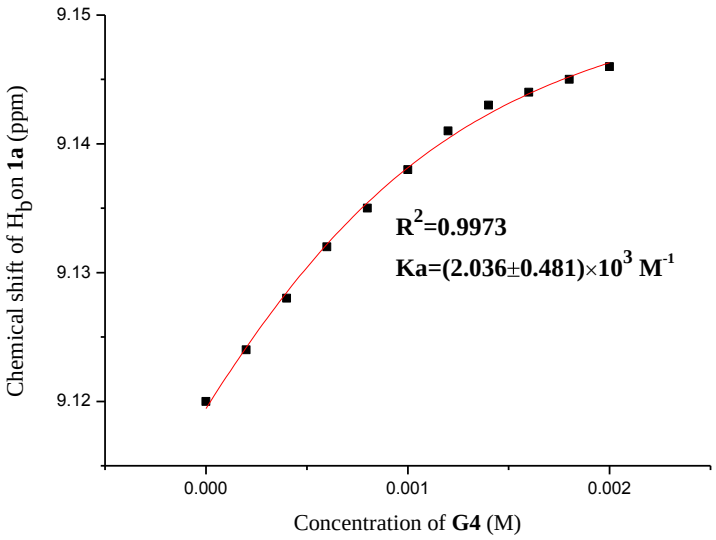

Figure S19. Determination of the binding constant of **1a•G4** in $CDCl_3$-CD_3OD (v/v, 9:1) at 298 K. Fitting result based on H_b of **1a**.

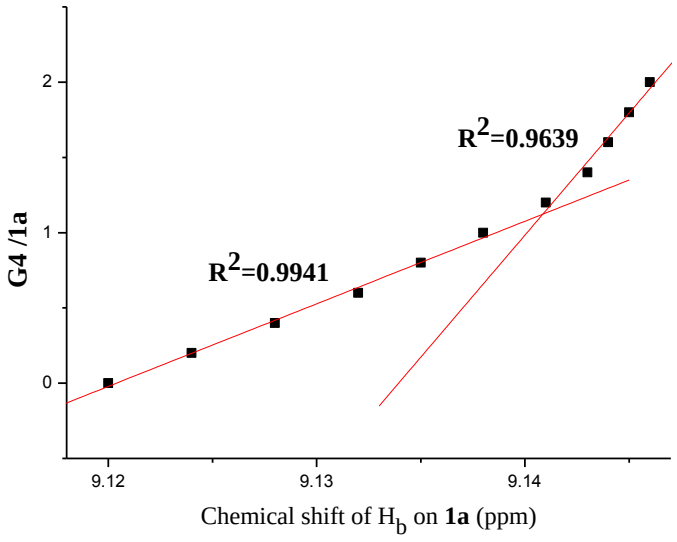

Figure S20. Mole ratio plot for the complexation between **1a** and **G4**, indicating a 1:1 stoichiometry.

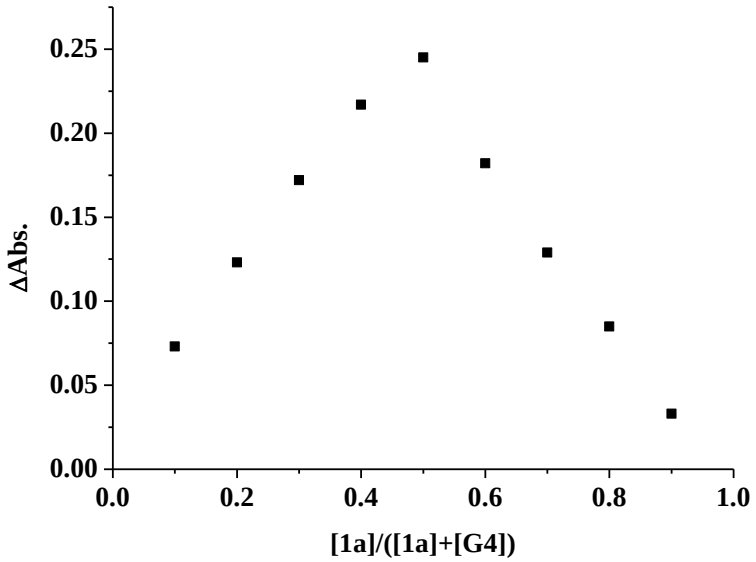

Figure S21. Job's plot for the complexation of **1a** and **G4** in $CDCl_3$-CD_3OD (v/v, 9:1) based on the absorbance at 365 nm, indicating a 1:1 stoichiometry. The total concentration is 3×10^{-4} M.

Table S6. The chemical shifts δ (ppm) for the 1:1 solution of **1a** and **G4** in $CDCl_3$-CD_3OD (v/v, 9:1).

Protons	**1a**	**1a**+**G4**	
	δ_f (ppm)	δ_b (ppm)	$\Delta\delta=\delta_b-\delta_f$ (ppm)
H_b	9.12	9.15	0.03
H_c	9.26	9.29	0.03

7. Host-guest complexation of 1a and TBACl

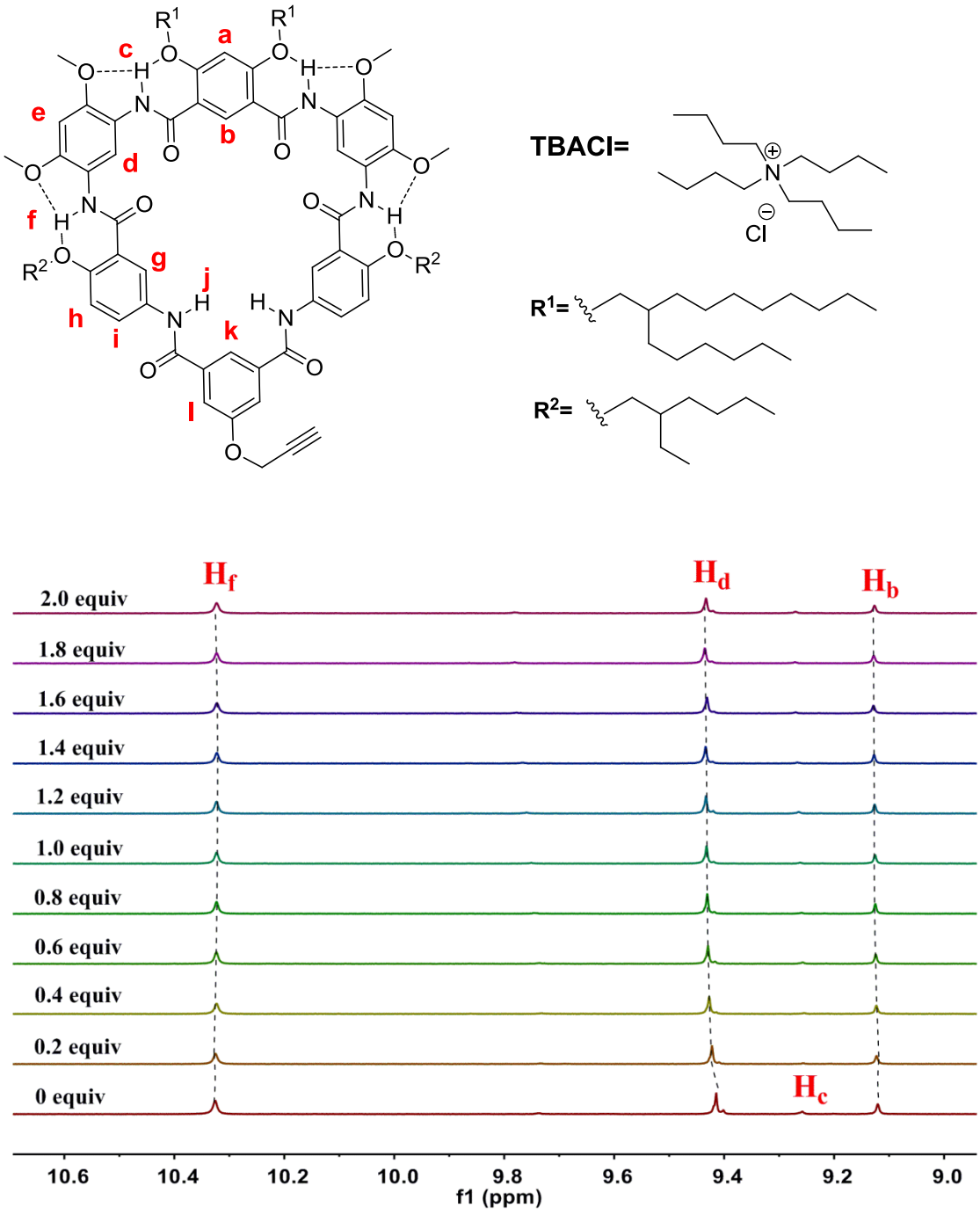

Figure S22. Partial stacked ^{1}H NMR spectra (400 MHz, 298 K) of cyclo[6]aramide **1a** (1.0 mM) titrated by **TBACl** (0-2.0 equiv) in $CDCl_3$-CD_3OD (v/v, 9:1).

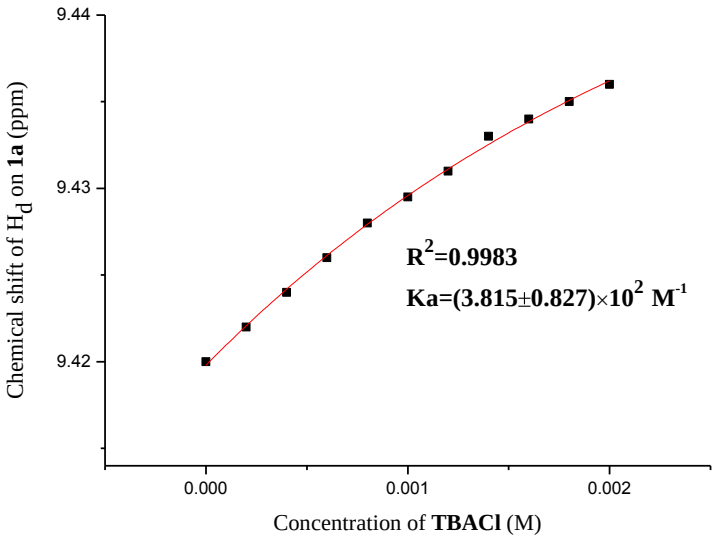

Figure S23. Determination of the binding constant of **1a•TBACl** in $CDCl_3$-CD_3OD (v/v, 9:1) at 298 K. Fitting result based on H_d of **1a**.

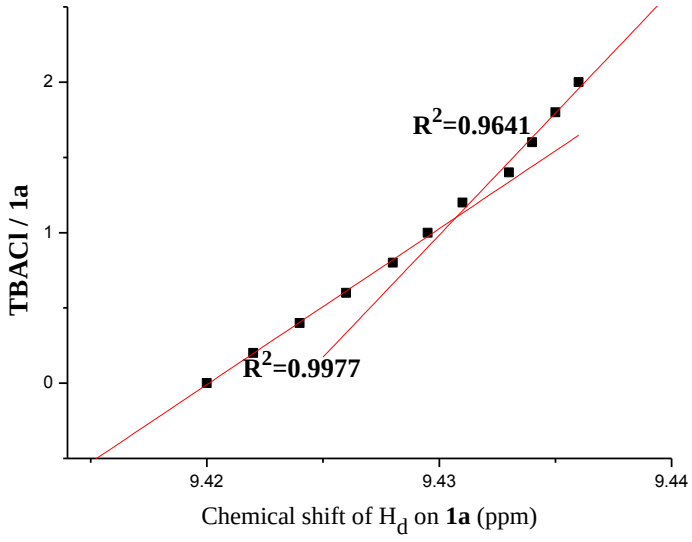

Figure S24. Mole ratio plot for the complexation between **1a** and **TBACl**, indicating a 1:1 stoichiometry.

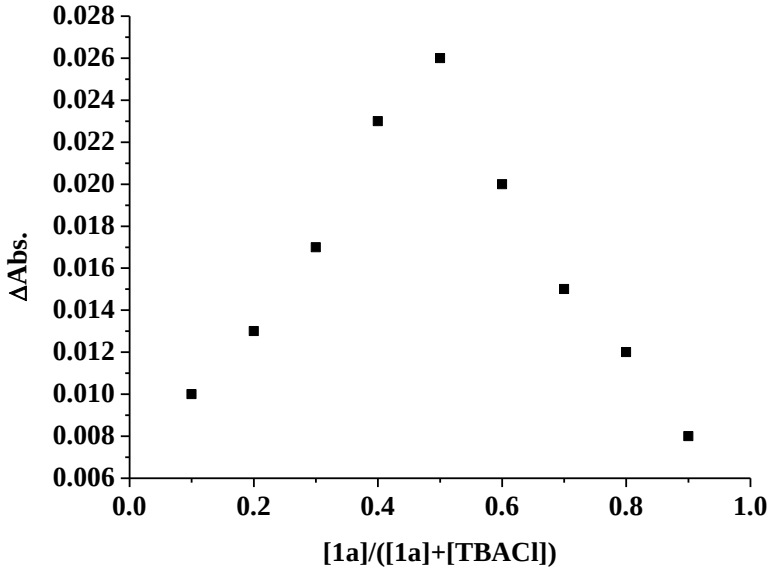

Figure S25. Job's plot for the complexation of **1a** and **TBACl** in $CDCl_3$-CD_3OD (v/v, 9:1) based on the absorbance at 365 nm, indicating a 1:1 stoichiometry. The total concentration is 3×10^{-4} M.

Table S7. The chemical shifts δ (ppm) for the 1:1 solution of **1a** and **TBACl** in $CDCl_3$-CD_3OD (v/v, 9:1).

Protons	**1a**	**1a**+**TBACl**	
	δ_f (ppm)	δ_b (ppm)	$\Delta\delta=\delta_b-\delta_f$ (ppm)
H_b	9.12	9.13	0.01
H_d	9.42	9.44	0.02

8. Host-guest complexation of 1a and G5

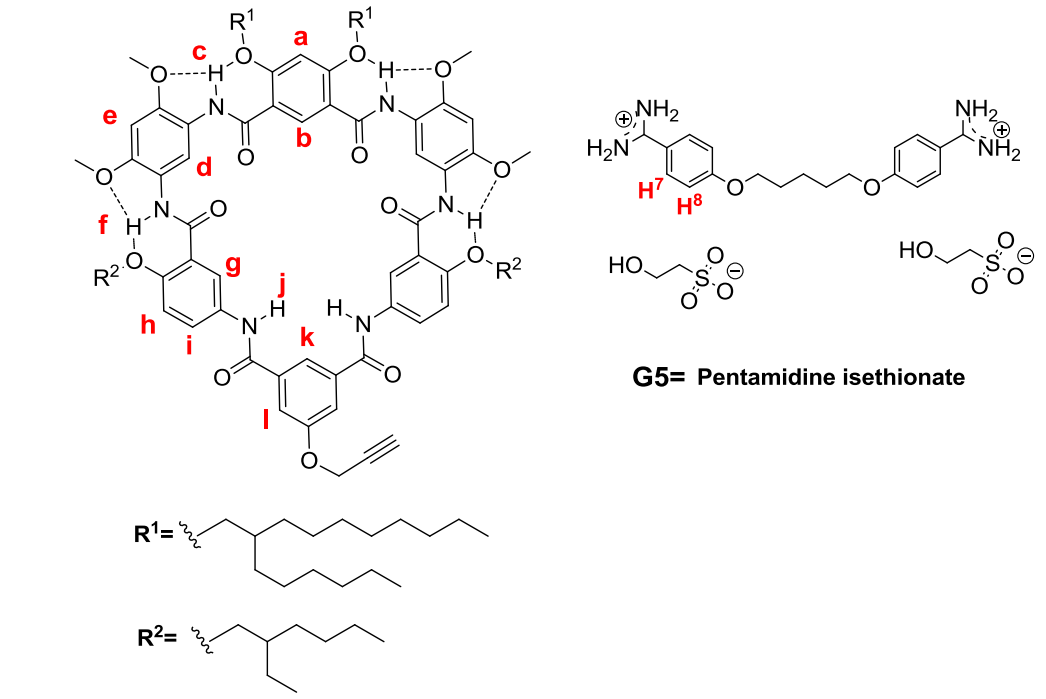

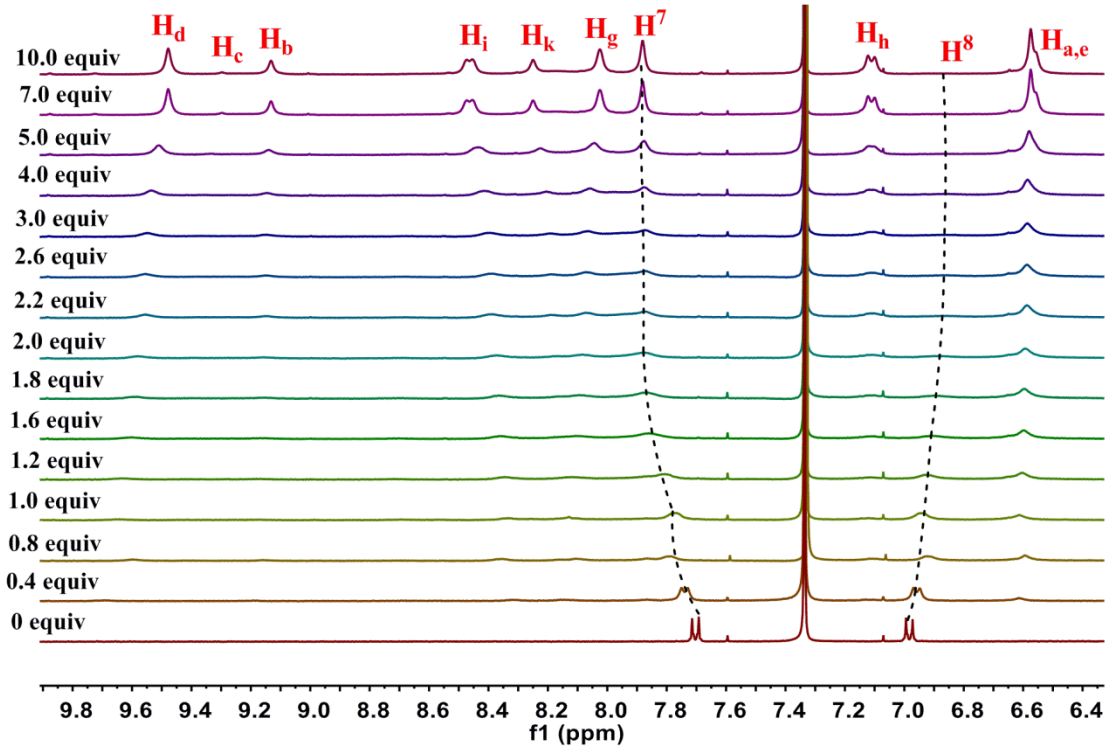

Figure S26. Partial stacked ^{1}H NMR spectra (400 MHz, 298 K) of **G5** (1.0 mM) titrated by cyclo[6]aramide **1a** (0-2.0 equiv) in $CDCl_3$-CD_3OD (v/v, 9:1).

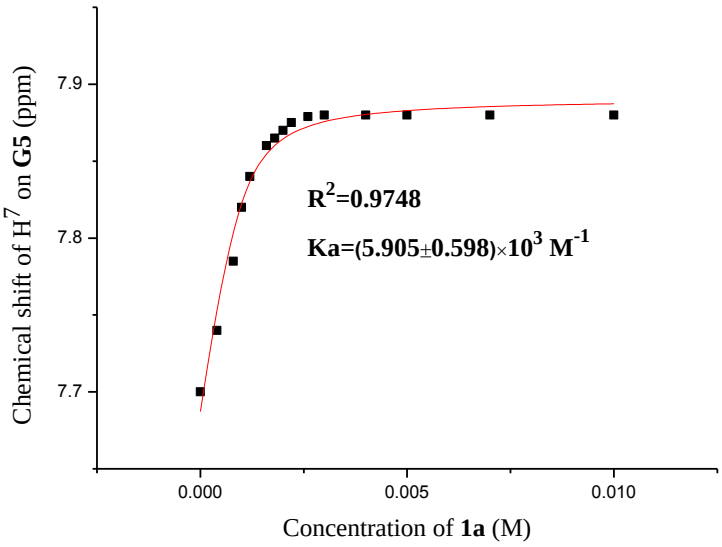

Figure S27. Determination of the binding constant of **1a•G5** in $CDCl_3$-CD_3OD (v/v, 9:1) at 298 K. Fitting result based on H^7 of **G5**.

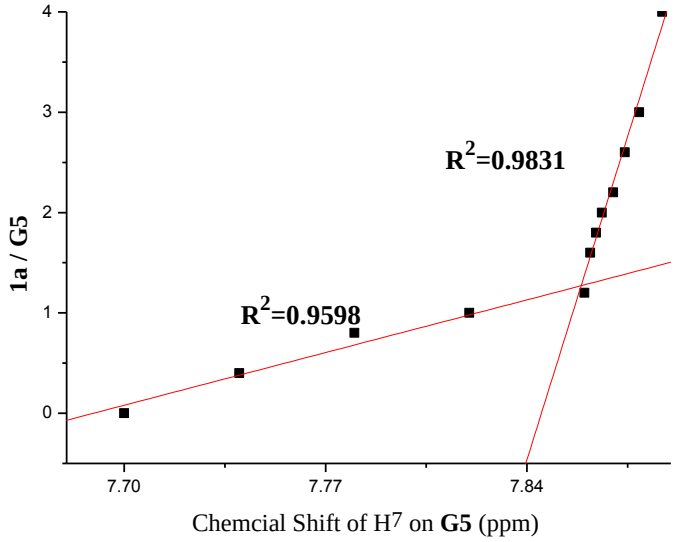

Figure S28. Mole ratio plot for the complexation between **1a** and **G5**, indicating a 1:1 stoichiometry.

Table S8. The chemical shifts δ (ppm) for the 1:1 solution of **1a** and **G5** in $CDCl_3$-CD_3OD (v/v, 9:1).

Protons	**G5**	**1a** +**G5**	
	δ_f (ppm)	δ_b (ppm)	$\Delta\delta=\delta_b-\delta_f$ (ppm)
H_7	7.69	7.88	0.18
H_8	6.99	6.85	–0.14

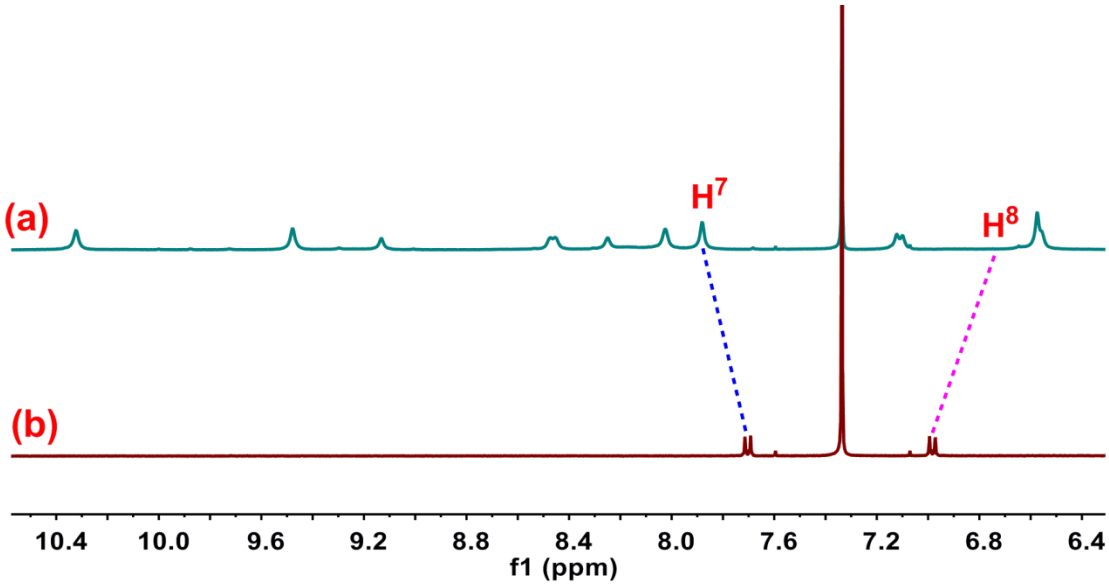

Figure S29. Partial ^{1}H NMR spectra (9:1, $CDCl_3$-CD_3OD, 298 K, 400 MHz) of (a) 5.0 mM cyclo[6]aramide **1a•G5**, (b) 1.0 mM **G5**.

9. HRESI-MS for complex

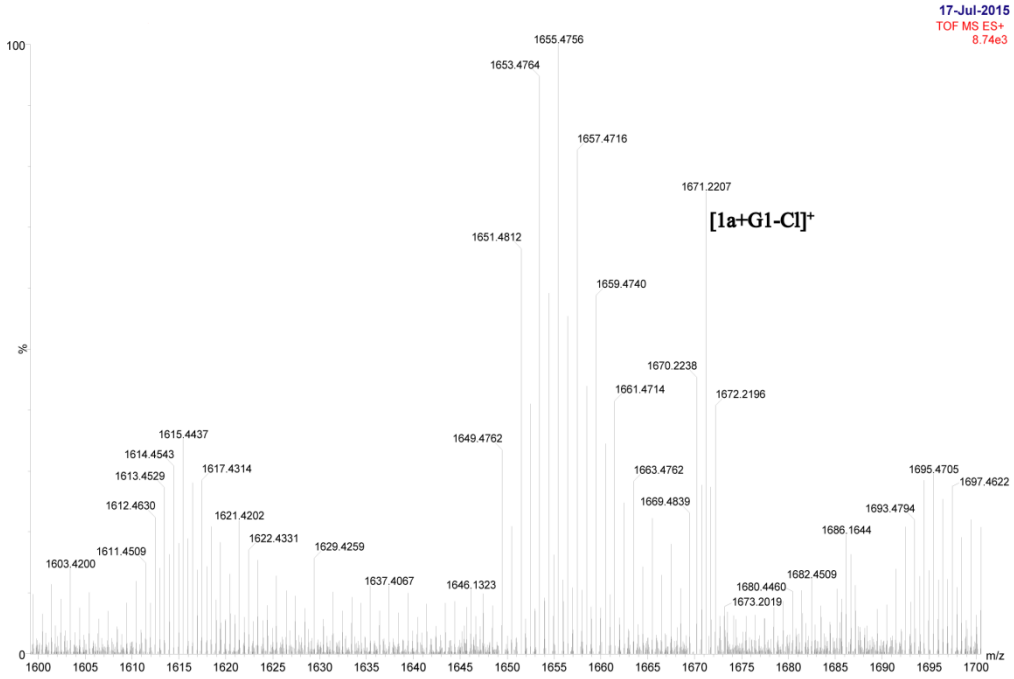

Figure S30. The HRESI-MS spectrum of an equimolar solution of **1a** and **G1** in methanol in the positive ion mode.

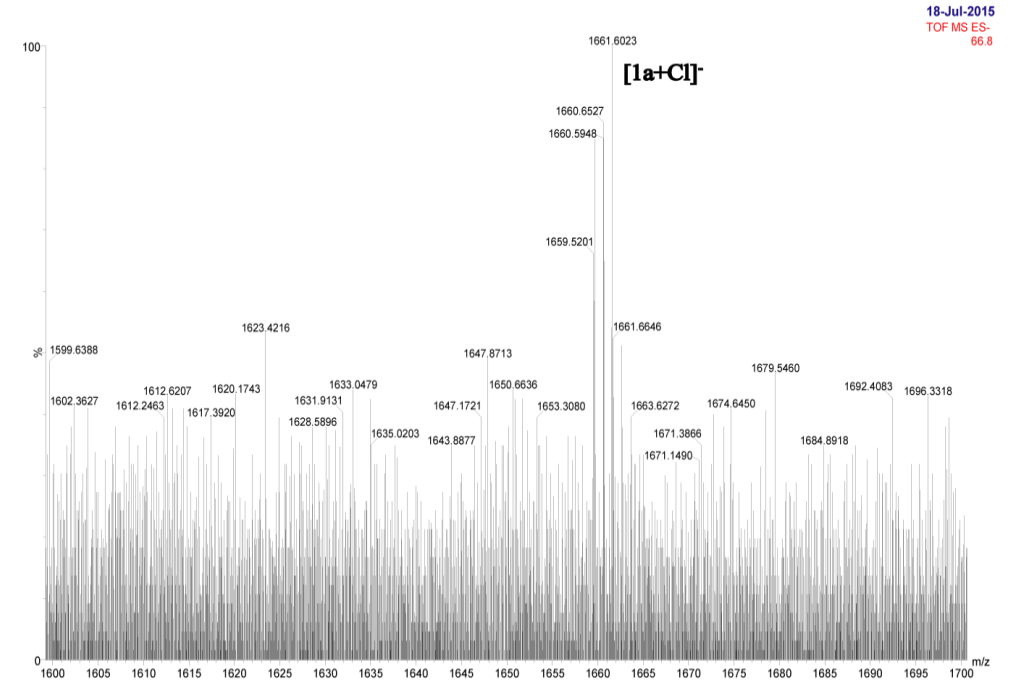

Figure S31. The HRESI-MS spectrum of an equimolar solution of **1a** and **G1** in methanol in the negative ion mode.

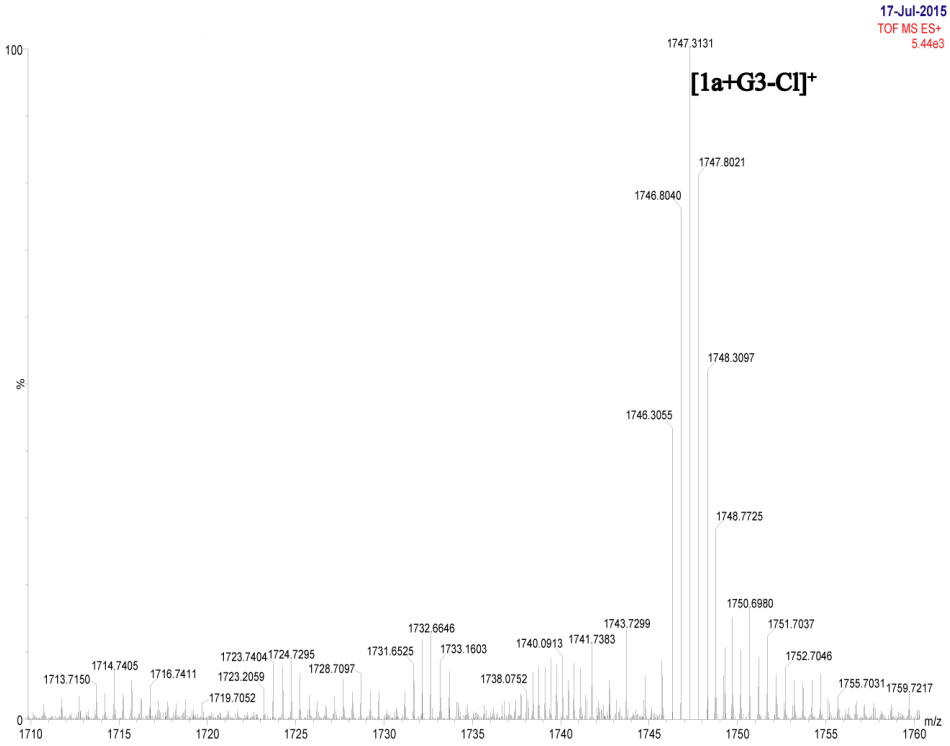

Figure S32. The HRESI-MS spectrum of an equimolar solution of **1a** and **G3** in methanol in the positive ion mode.

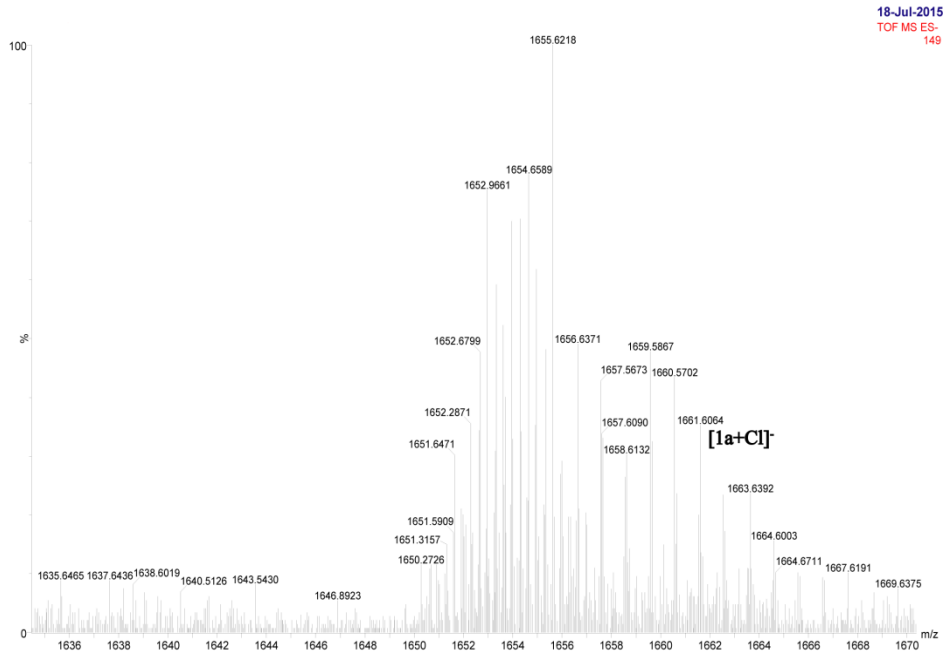

Figure S33. The HRESI-MS spectrum of an equimolar solution of **1a** and **G3** in methanol in the negative ion mode.

10.FT-IR transform infrared spectra of 1a and G1, G3

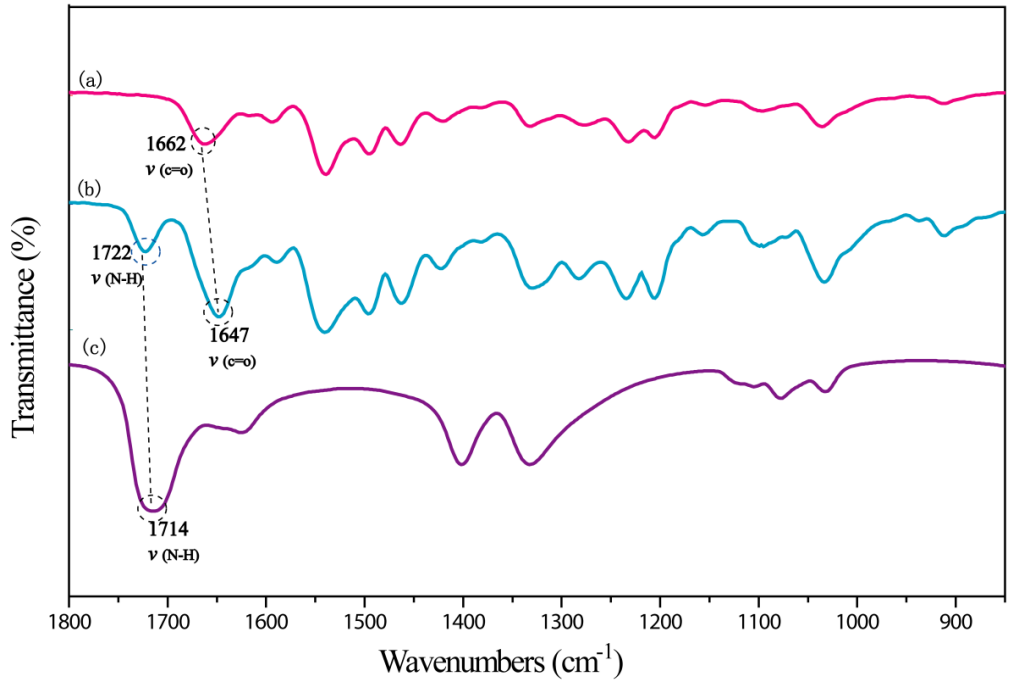

Figure S34. FT-IR transform infrared spectra of **1a** (a), complex **1a•G1** (b) and amidinium halide **G1** (c).

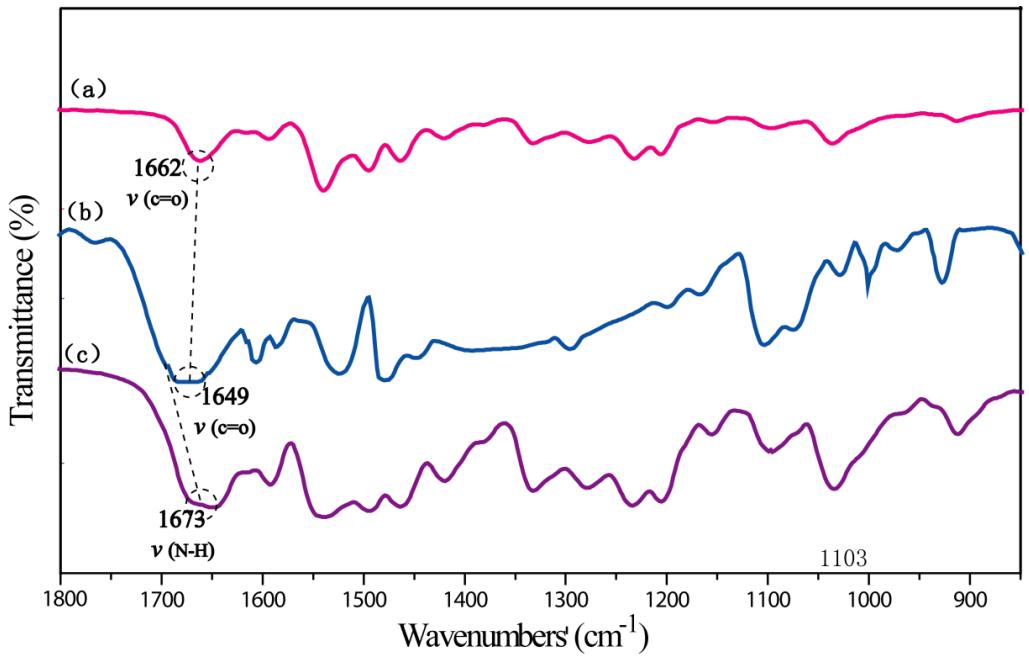

Figure S35. FT-IR transform infrared spectra of **1a** (a), complex **1a•G3** (b) and amidinium halide **G3** (c).

Table S9. The infrared wave numbers of (C=O) shifts ν (cm^{-1}) for the 1:1 solution of **1a** and **Guest** in solid.

Guest	**1a**	**1a+Guest**	
	ν_f (cm^{-1})	ν_b (cm^{-1})	$\Delta\nu=\nu_b-\nu_f$

			(cm^{-1})
G1	1662	1647	15
G2	1662	1648	14
G3	1662	1649	13

11. 2D NOESY spectrum of 1a•G2

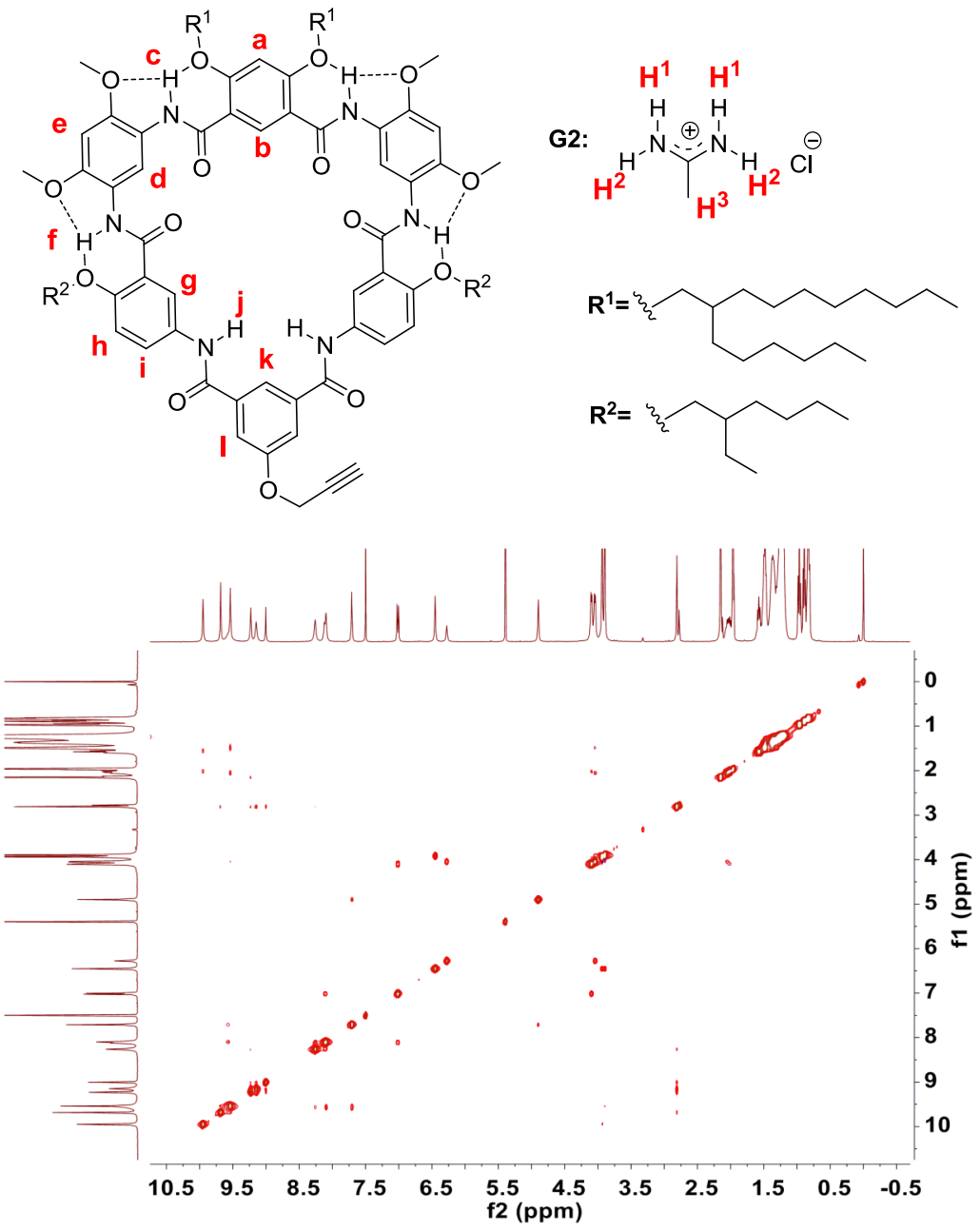

Figure S36. 2D NOESY spectrum (1:1, $CDCl_3$-CD_3CN, 400 MHz) between **1a** and **G2** (10 mM for each) at 298 K.

12. Electrical conductivity of guests and complex

The conductivity measurements were performed with a conductometer (DDSJ-308A, cell constant=1.0 cm^{-1}) with an uncertainty of 0.1%, and a dipping-type conductivity cell with platinised electrodes (DJS-1C) and under nitrogen atmosphere and at a fixed frequency of 1 MHz.[S5] The cell constant was obtained with aqueous KCl solution (10 mM). 5 mL of solution with mixed organic solvent (1:1, $CHCl_3$-CH_3CN, HPLC) containing different guests or complex (5 mM) was placed in the conductivity cell and the cell was closed. The temperature of the sample was maintained at 298.15±0.03 K with circulating water from a thermostatically regulated bath (Julabo, ED) around the sample holder with double wall. The specific conductance for mixed solvent is 0.9 μS cm^{-1}.

The electrical conductivities (σ) of the guest and complex at different concentrations are given in Table S8.

Table S10. The electrical conductivity σ values were obtained in $CDCl_3$-CD_3CN (v/v, 1:1) at 298 K.

	Guest	**1a+Guest**
	σ/μS cm^{-1}	σ/μS cm^{-1}
DBACl	63.4	52.3
DBAH	594.5	568.2

13. Molecular modelling of 1b with G1 and G2

The CT complex structure **1b•G1** was optimized by the density functional theory (DFT) method at the RB3PW91/6-31G (d, p) level by employing the Gaussian09 program.[S6]

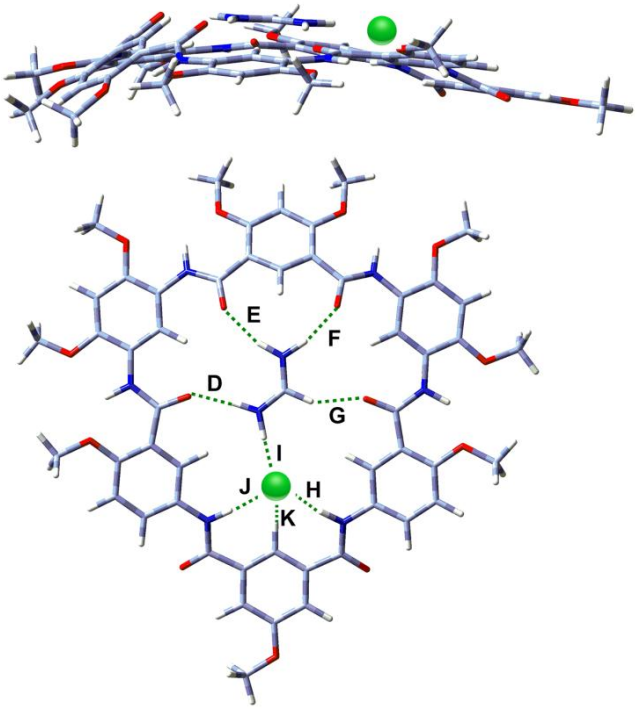

Figure S37. Side view a) and top view b) of optimized geometry of **1b•G1** at the RB3PW91/6-31G (d, p) level. The plane of **G1** is vertical to cyclo[6]aramide (gray = C, white = H, red = O and blue = N). All side chains are replaced by methyl groups for simplicity. The dashed green lines indicate intermolecular H-bonds **D-K** and with **D**= 1.888 Å, **E** = 1.965 Å, **F** = 1.889 Å, **G**= 2.311 Å, **H**= 2.283 Å, **I**= 1.982 Å, **J**= 2.308 Å and **K**= 2.464 Å.

Table S11. Atomic coordinates for the optimized structure of the complex **1b •G1**. The plane of **G1** is vertical to **1b**.

Center Number	Atomic Number	Atomic type	Coordinates (Angstroms)		
			X	Y	Z
1	6	0	5.049631	2.705688	-0.08548
2	6	0	3.278207	-4.69379	-0.08228
3	6	0	5.918264	3.801073	-0.17373
4	6	0	5.415647	5.080108	-0.3801
5	6	0	4.047387	5.309669	-0.49843
6	6	0	3.146827	4.224002	-0.40742
7	6	0	3.676309	2.942861	-0.2085
8	6	0	1.947588	-4.28466	-0.22712
9	6	0	0.899571	-5.1923	-0.42249
10	6	0	1.216404	-6.56782	-0.50149
11	6	0	2.539604	-6.97957	-0.36819
12	6	0	3.561887	-6.06301	-0.15587
13	6	0	1.647791	4.315255	-0.46017
14	8	0	0.954241	3.299811	-0.58081
15	7	0	1.101979	5.557154	-0.3099
16	6	0	-0.24931	5.90667	-0.19336
17	6	0	-0.48219	-4.59513	-0.47853
18	7	0	-1.52316	-5.47217	-0.32197
19	8	0	-0.64362	-3.37984	-0.60271
20	6	0	-2.88796	-5.19801	-0.1909
21	6	0	-0.53677	7.263608	0.062644
22	6	0	-1.8532	7.687647	0.236395
23	6	0	-2.90079	6.769355	0.15124
24	6	0	-2.62984	5.420123	-0.12112
25	6	0	-1.30739	5.004639	-0.28797
26	6	0	-3.45269	-3.92747	-0.2821
27	6	0	-4.82427	-3.73108	-0.1031
28	6	0	-5.65027	-4.82622	0.184095
29	6	0	-5.10234	-6.10725	0.26956
30	6	0	-3.73484	-6.29485	0.079858
31	7	0	-3.72088	4.530609	-0.12944
32	6	0	-3.72786	3.275247	-0.64513
33	6	0	-4.87989	2.375995	-0.29317

34	7	0	-5.41909	-2.45387	-0.10594
35	6	0	-4.91696	-1.34832	-0.70906
36	6	0	-5.49156	-0.01466	-0.32126
37	6	0	-5.98634	2.632526	0.541759
38	6	0	-6.83968	1.588775	0.920196
39	6	0	-6.58428	0.271285	0.521753
40	6	0	-4.72223	1.066608	-0.72786
41	8	0	-2.79504	2.830739	-1.32208
42	8	0	-3.95464	-1.39622	-1.48208
43	8	0	-7.3608	-0.77112	0.911996
44	8	0	-6.17963	3.91264	0.949753
45	6	0	-7.24422	4.213968	1.83651
46	6	0	-8.4489	-0.54437	1.792454
47	8	0	-6.97351	-4.53835	0.384044
48	6	0	-7.84956	-5.60824	0.665778
49	8	0	-3.11793	-7.511	0.148593
50	6	0	-3.90018	-8.64316	0.460375
51	8	0	-4.21927	7.085607	0.33517
52	6	0	-4.54901	8.430961	0.60655
53	8	0	0.54631	8.092029	0.132037
54	6	0	0.330082	9.457132	0.41801
55	8	0	0.192878	-7.45542	-0.71548
56	6	0	0.494062	-8.83084	-0.83644
57	8	0	3.528085	6.560892	-0.70667
58	6	0	4.412492	7.656404	-0.83645
59	7	0	5.497595	1.386575	0.103674
60	7	0	4.274356	-3.71966	0.111966
61	6	0	5.510972	-3.95603	0.654104
62	8	0	5.881833	-5.06612	1.031563
63	6	0	6.447954	-2.78226	0.750712
64	6	0	6.712488	1.036356	0.634643
65	6	0	7.011087	-0.43286	0.741483
66	8	0	7.552163	1.861034	0.994311
67	6	0	7.793815	-3.0998	0.918204
68	6	0	8.753922	-2.08884	1.004157
69	6	0	8.364138	-0.7553	0.91075
70	6	0	6.049709	-1.44102	0.687745
71	1	0	6.98186	3.644931	-0.06385
72	1	0	6.117492	5.902864	-0.44923
73	1	0	2.981433	2.114093	-0.13189
74	1	0	1.69821	-3.22967	-0.18074
75	1	0	2.795835	-8.03083	-0.42838
76	1	0	4.580273	-6.40215	-0.03156
77	1	0	1.757729	6.329974	-0.25476

78	1	0	-1.27346	-6.45449	-0.26922
79	1	0	-2.06176	8.728966	0.440884
80	1	0	-1.08964	3.971783	-0.49664
81	1	0	-2.80505	-3.09439	-0.4971
82	1	0	-5.73846	-6.95493	0.485305
83	1	0	-4.5671	4.855105	0.321484
84	1	0	-6.29063	-2.35863	0.399835
85	1	0	-7.69243	1.79943	1.550405
86	1	0	-3.90492	0.866291	-1.40146
87	1	0	-7.16852	5.28246	2.037835
88	1	0	-7.14842	3.659329	2.776975
89	1	0	-8.21628	4.000558	1.377116
90	1	0	-9.19835	0.11229	1.335768
91	1	0	-8.11052	-0.11656	2.743243
92	1	0	-8.89202	-1.52346	1.974072
93	1	0	-8.84299	-5.16952	0.772507
94	1	0	-7.86912	-6.33927	-0.15263
95	1	0	-7.58025	-6.11969	1.599421
96	1	0	-3.21338	-9.49016	0.48748
97	1	0	-4.38266	-8.54242	1.44127
98	1	0	-4.6673	-8.82726	-0.30305
99	1	0	-5.63516	8.465136	0.705075
100	1	0	-4.09177	8.780495	1.541559
101	1	0	-4.24499	9.093988	-0.21352
102	1	0	1.316055	9.922921	0.443925
103	1	0	-0.27536	9.941579	-0.359
104	1	0	-0.1553	9.593383	1.393067
105	1	0	-0.45831	-9.32779	-1.02532
106	1	0	0.938346	-9.23077	0.083439
107	1	0	1.172219	-9.01795	-1.67736
108	1	0	3.781481	8.527521	-1.01649
109	1	0	4.998624	7.81311	0.077367
110	1	0	5.09252	7.521159	-1.68563
111	1	0	4.883684	0.653284	-0.26916
112	1	0	4.056097	-2.78929	-0.26088
113	1	0	8.0903	-4.1405	0.985457
114	1	0	9.067892	0.066131	0.969768
115	1	0	5.000356	-1.18995	0.593883
116	6	0	11.04183	-1.51326	1.261051
117	1	0	11.09753	-0.90512	0.348648
118	1	0	10.87974	-0.84905	2.119972
119	1	0	11.98438	-2.04724	1.39349
120	8	0	10.04057	-2.50468	1.169403
121	7	0	-1.52587	0.163398	-1.47436

122	1	0	-1.78468	1.149225	-1.434
123	1	0	-2.28231	-0.51827	-1.52102
124	17	0	3.458871	-0.84456	-1.29708
125	7	0	0.769139	0.536269	-1.37202
126	1	0	0.712534	1.547865	-1.24239
127	1	0	1.712231	0.090688	-1.36037
128	6	0	-0.27315	-0.24086	-1.45018
129	1	0	-0.09996	-1.31575	-1.48665

The CT complex structure **1b•G2** was optimized by the density functional theory (DFT) method at the RB3PW91/6-31G (d, p) level by employing the Gaussian09 program.

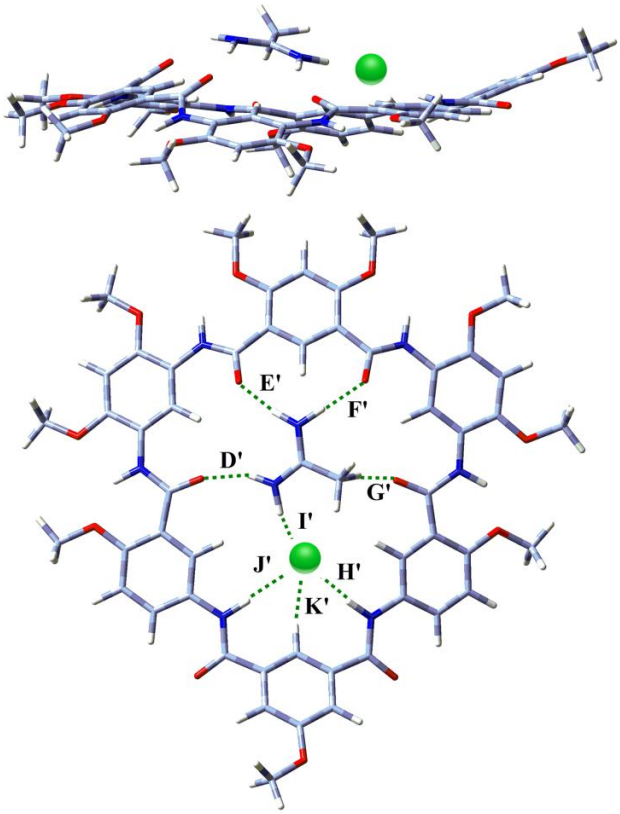

Figure S38. Side view a) and top view b) of optimized geometry of **1b•G2** at the RB3PW91/6-31G (d, p) level. The plane of **G2** is vertical to cyclo[6]aramide (gray = C, white = H, red = O and blue = N). All side chains are replaced by methyl groups for simplicity. The dashed green lines indicate intermolecular H-bonds **D′-K′** and with **D′**= 1.888 Å, **E′** = 1.965 Å, **F′** = 1.889 Å, **G′**= 2.311 Å, **H′**= 2.283 Å, **I′**= 1.982 Å, **J′**= 2.308 Å and **K′**= 2.464 Å.

Table S12. Atomic coordinates for the optimized structure of the complex **1b•G2**. The plane of **G2** is vertical to **1b**.

Center Number	Atomic Number	Atomic type	Coordinates (Angstroms)

			X	Y	Z
1	6	0	-5.20305	2.63862	-0.03367
2	6	0	-3.1733	-4.67536	-0.76561
3	6	0	-6.08018	3.725325	-0.15665
4	6	0	-5.58496	5.023302	-0.1995
5	6	0	-4.21976	5.28278	-0.12764
6	6	0	-3.31208	4.205489	-0.00821
7	6	0	-3.82956	2.906012	0.037558
8	6	0	-1.85435	-4.27703	-0.51164
9	6	0	-0.76054	-5.12638	-0.71913
10	6	0	-1.00646	-6.42423	-1.2218
11	6	0	-2.3129	-6.81652	-1.497
12	6	0	-3.38753	-5.96427	-1.27385
13	6	0	-1.81436	4.317435	0.069736
14	8	0	-1.12612	3.348617	0.402171
15	7	0	-1.27154	5.520262	-0.28681
16	6	0	0.079832	5.872568	-0.38048
17	6	0	0.588074	-4.53962	-0.39437
18	7	0	1.648309	-5.40717	-0.3654
19	8	0	0.704949	-3.33813	-0.15471
20	6	0	2.998537	-5.11277	-0.14908
21	6	0	0.375155	7.180058	-0.81817
22	6	0	1.698483	7.594143	-0.96546
23	6	0	2.743809	6.717056	-0.67282
24	6	0	2.462869	5.417728	-0.22452
25	6	0	1.134447	5.010507	-0.08886
26	6	0	3.503063	-3.83558	0.091882
27	6	0	4.872563	-3.6205	0.261141
28	6	0	5.762901	-4.69821	0.176583
29	6	0	5.273874	-5.98574	-0.05368
30	6	0	3.905039	-6.19394	-0.20904
31	7	0	3.554553	4.556935	-0.00673
32	6	0	3.515132	3.36209	0.635787
33	6	0	4.711909	2.465265	0.529517
34	7	0	5.413579	-2.3284	0.412422
35	6	0	4.776165	-1.26421	0.96657
36	6	0	5.363083	0.095699	0.711229
37	6	0	6.035772	2.787357	0.177303
38	6	0	7.00914	1.782904	0.104668
39	6	0	6.679089	0.445024	0.356055
40	6	0	4.438948	1.127239	0.781702
41	8	0	2.511316	2.962348	1.234049
42	8	0	3.706834	-1.36287	1.571622
43	8	0	7.584825	-0.56336	0.275912

44	8	0	6.307191	4.093483	-0.07762
45	6	0	7.626734	4.475841	-0.42591
46	6	0	8.928666	-0.26795	-0.06445
47	8	0	7.089356	-4.38801	0.30981
48	6	0	8.027856	-5.43736	0.21667
49	8	0	3.343453	-7.41842	-0.43518
50	6	0	4.184591	-8.55096	-0.44463
51	8	0	4.070724	7.02589	-0.80769
52	6	0	4.407984	8.30589	-1.29747
53	8	0	-0.70538	7.972794	-1.08056
54	6	0	-0.47744	9.275551	-1.57251
55	8	0	0.06606	-7.25382	-1.43073
56	6	0	-0.16013	-8.54231	-1.9641
57	8	0	-3.71175	6.556266	-0.15969
58	6	0	-4.60649	7.64706	-0.24527
59	7	0	-5.62915	1.302304	0.019425
60	7	0	-4.21552	-3.76957	-0.50206
61	6	0	-5.55787	-4.04397	-0.58093
62	8	0	-6.01502	-5.13524	-0.9153
63	6	0	-6.49448	-2.9304	-0.20606
64	6	0	-6.92752	0.865756	-0.04187
65	6	0	-7.13799	-0.61827	0.045254
66	8	0	-7.89882	1.615456	-0.13908
67	6	0	-7.74938	-3.32609	0.250585
68	6	0	-8.70381	-2.37223	0.610724
69	6	0	-8.39949	-1.01753	0.505017
70	6	0	-6.18934	-1.56923	-0.32856
71	1	0	-7.14326	3.541551	-0.21356
72	1	0	-6.29361	5.838381	-0.28824
73	1	0	-3.12676	2.083561	0.124109
74	1	0	-1.64984	-3.27628	-0.14154
75	1	0	-2.51802	-7.80523	-1.89044
76	1	0	-4.39628	-6.29143	-1.47893
77	1	0	-1.93	6.261585	-0.50241
78	1	0	1.447336	-6.37127	-0.60865
79	1	0	1.914086	8.597407	-1.30694
80	1	0	0.908893	4.014635	0.249447
81	1	0	2.811365	-3.01013	0.146338
82	1	0	5.957048	-6.82161	-0.11606
83	1	0	4.448892	4.866118	-0.36646
84	1	0	6.363112	-2.1886	0.092309
85	1	0	8.026334	2.042354	-0.15372
86	1	0	3.419706	0.85876	1.007487
87	1	0	7.593976	5.555121	-0.57375

88	1	0	7.952065	3.991969	-1.35437
89	1	0	8.332897	4.242956	0.379327
90	1	0	9.387957	0.39803	0.675106
91	1	0	9.00013	0.182011	-1.06174
92	1	0	9.452625	-1.22364	-0.06165
93	1	0	9.009971	-4.98204	0.354018
94	1	0	7.872808	-6.19	1.000524
95	1	0	7.994215	-5.92835	-0.76494
96	1	0	3.533639	-9.41328	-0.59481
97	1	0	4.915177	-8.50745	-1.26309
98	1	0	4.716384	-8.66632	0.508529
99	1	0	5.497664	8.339783	-1.34077
100	1	0	4.003582	8.474485	-2.30395
101	1	0	4.053697	9.100523	-0.62841
102	1	0	-1.46153	9.715913	-1.73793
103	1	0	0.073193	9.890774	-0.84903
104	1	0	0.070462	9.257566	-2.52342
105	1	0	0.824438	-9.00152	-2.06001
106	1	0	-0.63174	-8.48918	-2.95264
107	1	0	-0.78283	-9.15236	-1.29829
108	1	0	-3.98445	8.542767	-0.23507
109	1	0	-5.19068	7.619643	-1.17327
110	1	0	-5.28936	7.671107	0.61212
111	1	0	-4.90205	0.613485	0.24657
112	1	0	-3.93176	-2.87431	-0.09297
113	1	0	-7.98646	-4.38199	0.315498
114	1	0	-9.11015	-0.23886	0.753857
115	1	0	-5.23121	-1.25962	-0.72743
116	6	0	-10.8924	-1.92989	1.414682
117	1	0	-10.568	-1.29038	2.245992
118	1	0	-11.1818	-1.2923	0.569296
119	1	0	-11.7552	-2.51813	1.73157
120	8	0	-9.89589	-2.86206	1.051165
121	6	0	0.239657	0.013996	2.159272
122	7	0	1.460507	0.493546	2.375178
123	1	0	1.721918	1.432937	2.073577
124	1	0	2.220999	-0.17436	2.465473
125	6	0	-0.0122	-1.43246	2.433022
126	1	0	0.520674	-1.7423	3.334675
127	1	0	-1.08124	-1.62076	2.537491
128	1	0	0.354393	-2.02874	1.589298
129	17	0	-3.21909	-0.83325	0.858501
130	7	0	-0.74391	0.763072	1.729927
131	1	0	-0.6292	1.724567	1.414581

132	1	0	-1.64637	0.30118	1.505566

14. References

(S1) Hu, J. C.; Chen, L.; Shen, J.; Luo, J.; Deng, P. C.; Ren, Y.; Zeng, H. Q.; Feng W.; Yuan, L. H. *Chem. Commun.* **2014**, 50, 8024.

(S2) Gao, R. Z.; Hu, J. C.; Zhang, K.; He, Y. Z.; Liu, P.; Luo, S. Z.; Yang, Y. Q.; Yang, L.; Feng, W.; Yuan, L. H. *Chinese J. Chem*. **2013**, 31, 689.

(S3) Li, X. H.; Fang, Y. Y.; Deng, P. C.; Hu, J. C.; Li, T.; Feng, W.; Yuan, L. H. *Org. Lett.* **2011**, 13, 4628.

(S4) Kidd, T. J.; Leigh, D. A.; Wilson, A. J. *J. Am. Chem. Soc*. **1999**, 121, 1599.

(S5) B. Datta and M. N. Roy, *Phys. Chem. Liq*., **2015**, 53, 574.

(S6) Gaussian 09, Revision B.01, Frisch, M.J.; Trucks, G.W.; Schlegel, H.B.; Scuseria, G.E.; Robb, M.A.; Cheeseman, J.R.; Scalmani, G.; Barone, V.; Mennucci, B.; Petersson, G.A.; Nakatsuji, H.; Caricato, M.; Li, X.; Hratchian, H. P.; Izmaylov, A. F.; Bloino, J.; Zheng, G.; Sonnenberg,J.L.; Hada, M.; Ehara, M.; Toyota, K.; Fukuda, R.; Hasegawa, J.; Ishida, M.; Nakajima, T.; Honda, Y.; Kitao, O.; Nakai, H.; Vreven, T.; Montgomery, J.A., Jr.; Peralta, J.E.; Ogliaro, F.; Bearpark, M.; Heyd, J. J.; Brothers, E.; Kudin, K. N.; Staroverov, V. N.; Keith, T.; Kobayashi, R.; Normand, J.; Raghavachari, K.; Rendell, A.; Burant, J. C.; Iyengar, S.S.; Tomasi, J.; Cossi, M.; Rega, N.; Millam, J.M.; Klene, M.; Knox, J.E.; Cross, J.B.; Bakken, V.; Adamo, C.; Jaramillo, J.; Gomperts, R.; Stratmann, R.E.; Yazyev, O.; Austin, A.J.; Cammi, R.; Pomelli, C.; Ochterski, J.W.; Martin, R.L.; Morokuma, K.; Zakrzewski, V.G.; Voth, G.A.; Salvador, P.; Dannenberg, J.J.; Dapprich, S.; Daniels, A.D.; Farkas, O.J.; Foresman, B.; Ortiz, J.V.; Cioslowski, J.; Fox, D. J. Gaussian, Inc., Wallingford CT, **2010**.